Science of the Total Environment 806 (2022) 150499

Contents lists available at ScienceDirect

Science of the Total Environment

journal homepage: www.elsevier.com/locate/scitotenv

Thickness of peat influences the leaching of substances and greenhouse gas emissions from a cultivated organic soil

Markku Yli-Halla [a,*], Timo Lötjönen [b], Jarkko Kekkonen [b], Seija Virtanen [c], Hannu Marttila [d], Maarit Liimatainen [b,d], Markus Saari [d], Jarmo Mikkola [e], Raija Suomela [b,1], Erkki Joki-Tokola [b]

[a] Department of Agricultural Sciences, P.O. Box 56, FI-00014, University of Helsinki, Finland
[b] Natural Resources Institute, Paavo Havaksen tie 3, FI-90014, University of Oulu, Finland
[c] Drainage Foundation sr., Simonkatu 12 B 25, FI-00100 Helsinki, Finland
[d] Water, Energy and Environmental Engineering Research Unit, P.O. Box 8000, FI-90014, University of Oulu, Finland
[e] Natural Resources Institute, Latokartanonkaari 9, FI-00790 Helsinki, Finland

HIGHLIGHTS

- Loads of N, P, S, C and GHGs from an organic agricultural soil were monitored.
- Peat thickness increased N leaching.
- Dissolved P leaching increased upon increasing peat thickness.
- The peat layer seemed to slow down the oxidation of sulfidic material in the subsoil.
- CO_2 emissions were high and not significantly dependent on peat thickness.

GRAPHICAL ABSTRACT

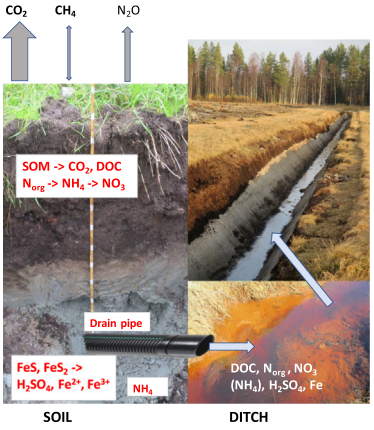

ARTICLE INFO

Article history:
Received 31 May 2021
Received in revised form 16 September 2021
Accepted 17 September 2021
Available online 23 September 2021

Editor: Ashantha Goonetilleke

Keywords:
Acid sulfate soils
AnaEE network
Nitrogen
Phosphorus
Organic carbon
Water quality

ABSTRACT

The off-site effects of agricultural organic soils include the leaching of N, P, and organic carbon (OC) to watercourses and CO_2, CH_4, and N_2O emissions into the atmosphere. The aim of this study was to quantify how the thickness of organic layers affects these loads. A 19.56-ha experimental field drained by subsurface pipes was established in Ruukki, northwestern Finland. Three plots had a 60–80 cm-thick sedge peat layer and three others had a thickness of 20 cm or less. The drainage pipes lie in mineral soil that, in this field, contains sulfidic material. This study documents the experimental settings and reports on the leaching of substances in the first two years, as well as CO_2, CH_4 and N_2O emissions during eight weeks in one summer. Total N (TN) and OC loads were higher from the thicker peat plots. The mean TN loads during a hydrological year were 15.4 and 9.2 kg ha^{-1} from the thicker and thinner peat plots, respectively, with organic N representing 36% of TN load. Total P (TP) load averaged 0.27 kg ha^{-1} yr^{-1}. Dissolved P load represented 63 and 36% of TP in the thicker peat area and only 23 and 13% in the thinner peat area, and was thus increased upon peat thickness. These N and P loads through the subsurface drainage system represented roughly 83% of TN and 64% of TP loads from this field. There were no clear differences in greenhouse gas emissions among the plots during the eight-week monitoring period. Slowly oxidizing sulfide in the subsoil

* Corresponding author.
E-mail address: markku.yli-halla@helsinki.fi (M. Yli-Halla).
[1] Present address: Oulu University of Applied Sciences, Yliopistokatu 9, P.O. Box 222, FI-90101 Oulu, Finland.

https://doi.org/10.1016/j.scitotenv.2021.150499

resulted in annual leaching of 147 kg S ha^{-1}, almost ten times that of non-sulfidic soils. Our first results emphasize the effect of the peat thickness on the leaching of substances and warn about considering all organic soils as a single group in environmental assessments.

1. Introduction

Globally, the organic soils of cool and humid climates form a major carbon (C) stock (Batjes, 1996; Scharlemann et al., 2014) and commonly serve as farmland (Berglund and Berglund, 2010; Buschmann et al., 2020). Many studies have highlighted the leaching of major nutrients and high greenhouse gas (GHG) emissions from cultivated organic soils (Duxbury and Beverly, 1978; Kasimir-Klemedtsson et al., 1997; Kløve et al., 2010; Tubiello et al., 2016; Regina et al., 2019). According to soil tests carried out in Finland between 1998 and 2002, 13.6%, or 300,000 ha, of agricultural land in the country consisted of organic soils (Myllys and Sinkkonen, 2004), and in the northern half of the country, almost 30% of agricultural land represented organic soils. They are mostly used for spring cereal and grass cultivation to provide fodder for dairy production (Kekkonen et al., 2019). The farming of organic soils is vital for local rural societies and food production, especially in north-western Finland. Therefore, there is a need for focused studies to accommodate the environmental challenges related to cultivation and to promote sustainable agricultural production.

According to the Intergovernmental Panel on Climate Change (IPCC, 2014), "organic soil" has at least a 10-cm thick horizon consisting of material that, when mixed to the depth of 20 cm, has at least 12–18% organic carbon (i.e., at least 20–30% soil organic matter (SOM), depending on the clay content). This definition matches well with the traditional Finnish criteria, where organic soils are principally divided into two categories (i.e., 1) peat soils that have ≥40% organic matter and 2) other organic soils that contain 20–39.9% of organic matter ("mull soils") in the plough layer, often with a mineral subsoil). These criteria are applied to the plough layers of agricultural land, with no other depth requirements. Many of the soils in the mull category have been formed either as a result of the ploughing of shallow peat soil, mixing the topsoil peat with the mineral subsoil, or by a decrease of the organic matter content of the original peat soil due to long-term cultivation. These definitions differ from the criteria of the Histosols of Soil Taxonomy (Soil Survey Staff, 2014) or the World Reference Base for Soil Resources (IUSS Working Group WRB, 2014), where, in an agricultural context, at least a 40-cm thick horizon consisting of organic material is required. Many Finnish mull soils thus belong to the mineral soil classes of Soil Taxonomy or WRB, with a shallow histic horizon.

Organic soils are usually located in flat parts of the landscape where water-logged conditions have favored the growth of mosses or sedges and the formation of peat. Wetness prevents organic matter oxidation and stores it as peat (e.g., Maljanen et al., 2007). When reclaimed for agriculture, these soils need to be artificially drained, which leads to the aerobic decomposition of organic matter coupled with N mineralization. Before being productive, these fields usually require liming, which promotes microbial activity and further enhances decomposition (Ivarson, 1977). Tillage also enhances decomposition via an increased aeration of the soil. Thus, agricultural use has various effects through which organic matter is lost from organic soils. Nitrogen is first released as ammonia upon mineralization, and part of it is consumed by plants and other organisms, while other parts (especially nitrate) can be leached to the drainage system and further to surface waters. Transport of C and N from the soil also takes place in the form of humic substances that are dissolved or suspended in drainage water (Mattsson et al., 2005; Manninen et al., 2018). As for emissions into the atmosphere, fluxes of carbon dioxide (CO_2) and nitrous oxide (N_2O) increase upon agricultural use of organic soils whereas methane (CH_4) emissions commonly decrease (Maljanen et al., 2007).

On the flat western coast of Finland, the land is still emerging from the sea as a consequence of post-glacial rebound following the Weichselian glaciation that ended about 10,000 years ago; the annual rebound is about 2 mm in the south and 8 mm in the northern part of the coast (Tikkanen and Oksanen, 2002). Thus, the time for the accumulation of peat has been rather short on these coastal areas. Soil surveys conducted about 50 years ago (Soini and Virri, 1968; Urvas, 1976) documented that sedge peat was the most common soil type of agricultural land in many areas of Ostrobothnia on the western coast of Finland, and the horizons that consist of organic material were thin. Even though the SOM content of the plough layer may be as high as 60% (organic carbon 35%) (Soini and Virri, 1968), the total SOM stock can be rather small, owing to the shallow depth of the organic material. In these soils, the subsurface drainage pipes, usually installed at depths of 1.2 m, lie almost exclusively in the mineral soil layers. However, the only experimental field where the leaching of nutrients from an organic soil has been monitored in Finland represents a soil that has a deep (3–4 m) peat layer (Huhta and Jaakkola, 1993), and it is questionable whether or not those results can be extrapolated to thin organic soils. In addition, the thickness of organic horizons has not been explicitly considered in studies where GHG emissions have been measured.

Organic matter as such possesses a low capacity to retain dissolved phosphorus (P); therefore, cultivated organic soils can be sources of P loading to waters (Longabucco and Rafferty, 1989; Huhta and Jaakkola, 1993). However, organic soil material commonly contains plenty of mineral material and associated iron (Fe) and aluminum (Al) oxohydroxides which can effectively retain P. The P retention capacity of peat samples is also strongly dependent on the concentration of Fe and Al (Kaila, 1959; Nieminen and Jarva, 1996; Ronkanen et al., 2016). Phosphorus leaching from organic soils likely depends on whether subsurface pipes have been installed in the mineral or organic subsoil. Therefore, the thickness of the organic horizons probably has an impact on P leaching as it influences water flow paths.

Besides peat soils, acid sulfate (AS) soils are also prevalent on the western coast of Finland (Purokoski, 1959; Yli-Halla et al., 1999; GTK, 2021). Organic soils in that area commonly have fine- or medium-textured AS subsoils that contain sulfidic material. The subsoils have been partly oxidized upon artificial drainage, resulting in acidification of the soil and drainage water (Edén et al., 1999; Beucher et al., 2015). Studies carried out in peat mining areas have shown that a peat layer thicker than 0.5 m may inhibit the oxidation of sulfidic materials of the deeper horizons (Nystrand et al., 2019); however, the effect of peat thickness on acid loadings has not been studied in cultivated subsurface drained peat fields. In these kinds of fields, in addition to the decomposition of peat, a substantial load of N can be produced by the oxidation of the large mineral N stock in the subsoil (Yli-Halla et al., 2020). Therefore, the N load from organic soils that contain sulfidic material in the subsoil can originate from the mineralization of SOM in the upper soil horizons and the AS horizons deeper in the soil.

Accurate information concerning nutrient loads and GHG emissions from shallow agricultural peat soils is needed when developing policies for the sustainable use of organic soils. The primary aim of this study was to quantify the loads of N, P, acidity and total organic carbon (TOC) into the watercourses and GHG emissions into the atmosphere from a shallow agricultural sedge peat soil with an AS subsoil, a set of characteristics typical of the western coast of Finland. In this study, we document the characteristics of a newly established experimental field at the Ruukki field station and report on hydrology and the leaching of substances during the first two hydrological years after establishing

the field. GHG emissions were measured in one summer. We hypothesized that the thickness of the peat layer affects leaching and atmospheric emissions from the peat fields 1) in terms of P leaching— shallow peat soils differ from thick peat soils and behave more like mineral soils, retaining P strongly onto the abundant Fe and Al oxide surfaces; 2) the thickness of the peat layer affects N and TOC loads to discharge water; 3) GHG emissions into the atmosphere are increased upon increasing peat thickness; and 4) the acidity released from the subsoil is related to the thickness of the peat layer.

2. Materials and methods

2.1. Experimental field and weather observations

The experimental field is located at the Ruukki research station (25.00°E, 64.42°N) in the Siikajoki municipality, about 60 km southwest of Oulu, Finland (Fig. 1A). Its elevation is circa 45 m above the mean sea level, and the distance from the current seashore is 26 km. The station belongs to the Natural Resources Institute Finland (Luke). The current experimental field was established in 2016 to allow monitoring of GHG emissions and the leaching of substances. The surface soil is sedge peat, mixed with different amounts of coarse silt, and the subsoil consists of actual and potential AS soil material. The present experimental area was already entirely in agricultural use about 100 years ago, as proven by a soil map drawn in 1933. The experimental field has an area of 19.56 ha, divided into six plots, 2.97–3.77 ha each (Fig. 1B), and it has a slope of less than 0.5%. The field belongs to the European network of platforms for Analysis and Experimentation on Ecosystems (AnaEE, 2021).

The average annual temperature at Ruukki between 1981 and 2010 was 2.6 °C, with January being the coldest (−9.3 °C) and July the warmest (15.9 °C) month. The average precipitation during the same 30-year period was 541 mm. Snow cover in the area usually lasts from late November until mid-April, about 130–140 days. The growing season (daily mean temperature > 5 °C) commonly starts in the first days of May and ends at the beginning of October (Kersalo and Pirinen, 2009; Finnish Meteorological Institute, 2021). Air temperature and precipitation data for the present monitoring period were obtained from the Finnish Meteorological Institute which has a weather station 800 m from the midpoint of the experimental field. The depth of the frozen ground was measured monthly using methylene blue tubes where the color change indicates the depth of frost (Soveri and Varjo, 1977).

2.2. Soil chemical properties and spatial variation of peat thickness

Before setting up the experimental field, the area was surveyed for the thickness of the peat layer, sampled at depths of 0–40 cm, 40–80 cm and 80–100 cm and analyzed for pH at a soil-to-water ratio of 1:2.5 using a Radiometer GK 2401B electrode. The electrical conductivity (EC) of the supernatant was measured with a ProMinent Dulcotest TyP LFT 1 FE electrode. Easily soluble calcium (Ca), magnesium (Mg), potassium (K), P, and sulfur (S) were extracted with a mixture of 0.5 M ammonium acetate and 0.5 M acetic acid solution buffered at pH 4.65 (Vuorinen and Mäkitie, 1955), which is the soil testing method used in Finland. Phosphorus concentration was measured colorimetrically with a Foss – Tecator FIAStar 5000 Flow Injection Analyser, while Ca, Mg, K, and S were measured with an ICP-OES Thermo Fisher Scientific iCAP6500 Duo Inductively Coupled Plasma Optical Emission Spectrometer.

In Plot 3 and a few meters from the edge of Plot 6, drillings extending to the depth of 3 m (drilling sites P1 and P2 in Fig. 1B) were made by the Geological Survey of Finland during a survey of acid sulfate soils (GTK, 2021). Mineral subsoil samples were analyzed at intervals of 20 or 40 cm for total S after aqua regia digestion. Subsoil samples were tested for sulfidic material measuring the fresh pH(H_2O) right after sampling and after eight weeks of aerobic incubation using a Hamilton Flatrode electrode and a minimal amount of water. To meet the definition of sulfidic material, soil pH has to drop at least 0.5 pH units to a final pH value of 4.0 or less during the incubation (Soil Survey Staff, 2014). Eleven additional drillings (locations not shown, distributed evenly) were made within and in the vicinity of the plots to the depth of 2 m, to visually assess the textural class and the depth of sulfidic material.

A ground penetrating radar (GPR) survey to determine the depth of the organic horizons was conducted in July 2020. The GPR lines with a total length of 17 km form an even grid with a transect gap of 30 m. The setup for measurement consisted of a Malå Geoscience ProEx unit with a 250 MHz shielded antenna. The data were validated with 32 manual depth measurements. Data were processed and interpreted using ReflexW software (Sandmeier, 2016).

The soil layers consisting of organic material (thickness 20–80 cm at different plots) were sampled in the middle of every plot between the laterals (subsurface drainage pipes that conduct water to the collector pipes) at intervals of 10 cm. Below the organic material, the uppermost 10 cm of the mineral subsoil and the deeper mineral soil layers at intervals of 50 cm were also sampled. These samples were analyzed for total C and N using a Leco CHN628 or Leco TruMac CN dry combustion apparatus. To calculate the C and N stocks, bulk density was determined with a core method using 150 cm^3-cylinders with individually determined volumes. The soil of each plot was classified according to the WRB system (IUSS Working Group WRB, 2014).

Additional soil samples were taken at 0–20, 20–50, 50–100, 100–120 (or 150) and 150–200 cm in the middle of every plot in May 2020 before fertilization. The soil samples were stored frozen until mineral N (Nmin) was extracted with 2 M KCl (Esala, 1995). The concentrations of ammonium-N (NH_4^+-N) and nitrate-N (NO_3^--N) were determined colorimetrically with an autoanalyzer (Lachat QuickChem AE, Hach, Loveland, CO, USA or Skalar San++ System, Skalar Analytical B.V., Breda, The Netherlands).

2.3. Cultivation of the experimental field

The crops and agricultural practices are presented in Supplementary Table S1. Grasses harvested for silage and cereals were grown in the field. In 2016, when the experiment was established, the whole field was under a mixture of timothy and meadow fescue grass. In spring 2017 basic slag was applied at a rate of 8 tons per ha to decrease soil acidity, and the field was seeded with cereals. Plots 5 and 6 were undersown with grass seeds simultaneously with the sowing of cereal. The aboveground vegetation was harvested as whole-crop silage in September. In summer 2018 spring barley for grain was grown in Plots 1–4 and the grass was harvested as silage in Plots 5 and 6. The fertilization was carried out with compound NPKS and NPS fertilizers. The ley received surface application while the fertilizers for cereals were drilled into the soil. All farming activities were carried out using conventional farm machinery.

2.4. Land drainage of the experimental field

The experimental plots were originally drained by open ditches. Subsurface drainage was subsequently installed, using wooden box drains in 1900 (Plot 6), clay pipes in 1960 (Plot 5) and plastic pipes in the 1980s (Plots 1 and 2). The subsurface drainage was renewed with plastic pipes in the 1980s (Plots 1 and 2), in 2005 (Plots 5 and 6), and in 2007 (Plots 3 and 4). For this experiment, the existing subsurface drainage was largely used in Plots 3, 4, 5, and 6, to avoid unnecessary disturbance of the soil. It is known that during the first few years after the installation of subsurface drainage, elements can be mobilized because of soil disturbances during trenching (Äijö et al., 2016), which may also promote the oxidation of sulfidic material and consequent acidification in AS soils.

In Plots 1 and 2, new subsurface drainage had to be installed because the old drainage did not function well. Owing to the gradual oxidation

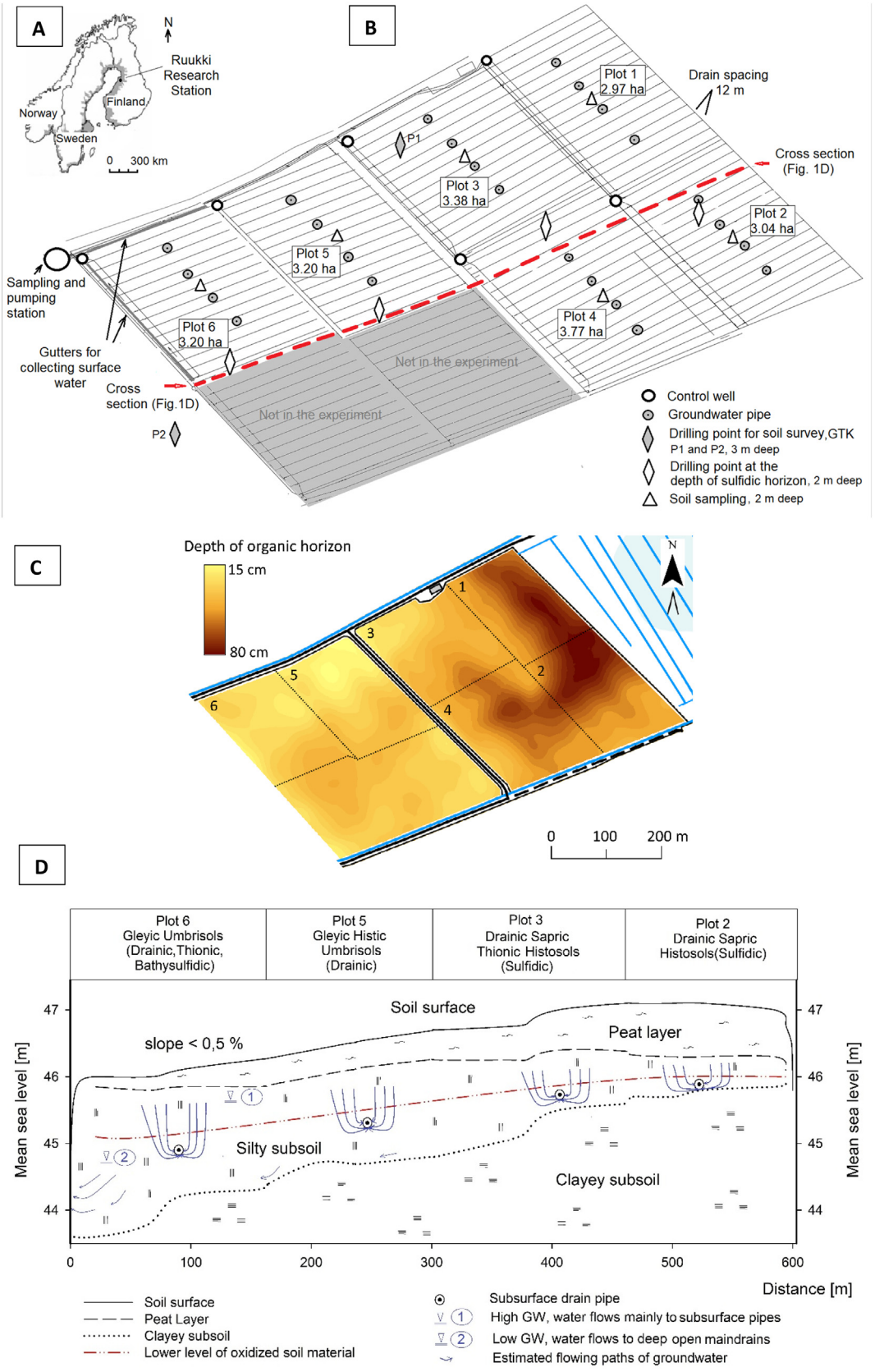

Fig. 1. A) The location of the Ruukki experimental station. The shaded area shows where acid sulfate (AS) soils can potentially exist in Scandinavia. B) The drainage and soil survey map of the experimental field. C) The thickness of the organic horizons. D) Schematic cross sectional drawing of the experimental field.

and compaction of the surface peat, the drainpipes were only at a depth of 80 cm. The laterals (corrugated PVC pipes, Ø 65 mm) were installed at a depth of 1.1–1.3 m, with a drain spacing of 12 m. Gravel (0.2–4 mm) was used about 6.5 m^3 per 100 m above the drainage pipes. The laterals were connected to collectors (diameter Ø 160 mm) that convey the waters to a control well (Ø 800 mm, height 1800 mm) in the corner of each plot. The groundwater level of the plots can be controlled by adjusting the height of the outlet pipe in the control well, but during the monitoring period in this study, the control system was not in use. From each control well, a separate outlet pipe conveys water to the sampling station at the lower end of the field. In this area, rust precipitates constantly clog the drainage pipes; therefore, every lateral has a joint tubing that extends to the soil surface and can be used for flushing rust out of the pipes.

To prevent the ponding of water on the soil's surface, the depressions within the plots were levelled with an RTK-GPS steered grader during autumn 2016 and spring 2017. The target was to carry out grading so that every plot inclines to the edges of the field. Plot 6 was levelled so that its inclination was marked toward the two surface runoff gutters in the corner (Fig. 1B) from where the runoff is channelled into the sampling station. This arrangement appeared not to be functional during the snowmelt periods, and the measured surface runoff remained low. Therefore, the surface runoff gutters were replaced in 2019, and preliminary results of the surface runoff volumes of 2020 were obtained for this paper.

2.5. Monitoring of groundwater level and drain discharge

Perforated groundwater (GW) pipes (diameter Ø 50 mm) were installed in each field reaching a depth of 2 m. In all, four pipes were installed to each plot between the laterals. The GW levels were monitored manually from all pipes between July 5 and August 28, 2017 and continuously (at 15-min intervals) using Solinst Levelogger sensors installed in two pipes at each plot between March 26 and December 31, 2018. The drain discharge was collected at the sampling station from each plot individually, and the water volume was measured using a V-dam and water pressure sensor (type: STS PTM/N) (Supplementary Fig. S1A–D). These data were collected on-line and stored in a cloud service, so it could be viewed via the internet. The runoff ratio (RR) was calculated individually for the plots by dividing the discharge amount of the respective plot by the precipitation measured for the Ruukki station.

Discharge water needs to be pumped away from the sampling station, because the water level outside the station is often higher than the outlets for sampling. The theoretical design flow for the whole area (19.56 ha) is 20 l s^{-1}. The electrical discharge pump (2.5 kW) was chosen so that its capacity would be enough to pump away the whole design flow. However, during times of extremely high flow, there has been flooding in the sampling station, and a tractor-driven hydraulic pump was used for flood control. Sampling pumps, sampling cans, and command electronics were all placed above the flood line.

The discharge waters are rich in dissolved Fe, and rust tends to precipitate onto the lower corner of the V-dam opening, resulting in erroneous results of the discharge volume. Therefore, a system was developed to remove the precipitates at intervals of 6 h automatically with pressurized (3–4 bar) air.

2.6. Water quality measurement

Water samples were automatically taken by hose pumps proportional to the discharge volume. About 0.1-liter subsamples were drawn into 10-liter cans from every 2000 l of drainage water. From every plot, 1 l of the collected water was delivered to a laboratory for periodic analysis in 2016–2017. In 2018, the samples were stored in a freezer at −20C° until analyzed in spring 2019. According to Dore et al. (1996) and Fellman et al. (2008), the freezing of water samples does not have a marked effect on the concentrations of elements that we measured. Altogether, 23 water samples from each plot were taken between October 2016 and October 2018. The samples represented the periods of rainy autumn plus early winter and snow melt in spring. During the discharge periods, the intervals between samplings were 5–29 days, with a mean of 12 days. Hydrological years, starting in October, are used as the basis for presenting the flow-weighted characteristics of water samples and substance loads.

The electrical conductivity (EC) of water samples was measured with a conductivity meter (SFS-EN 2788:1994). The pH was measured according to SFS 3021:1979. Acidity was analyzed with a potentiometric titration with 0.02 M sodium hydroxide (NaOH) up to pH 8.3 (SFS 3005:1981). Total organic carbon (TOC) was determined according to SFS-EN 1484:1997 using a Shimazdu TOC-LCSH analyzer where the CO_2 generated by oxidation is detected using an IR gas analyzer. Sulfur was analyzed with the method SFS-EN ISO 11885:2009 from unfiltered samples acidified with nitric acid (HNO_3) using a Thermo Fisher Scientific iCAP6500 Duo Inductively Coupled Plasma Optical Emission Spectrometer. Phosphorus was determined colorimetrically using a Foss – Tecator FIAStar 5000 Flow Injection Analyser (FIA) (SFS-EN ISO 15681-1:2005). For total P, unfiltered samples were digested with peroxodisulfate before determination, and for dissolved P determination, the original samples were filtered using 0.45 μm Polyethersulfone (PES) filters. Particulate P was calculated as the difference of total P and dissolved P. Total N was measured colorimetrically with FIA after an oxidative digestion with peroxodisulfate (ISO 11905-1:1997). Concentrations of NH_4^+-N and NO_3^--N were determined colorimetrically with FIA according to SFS-EN ISO 11732:005 and SFS-EN ISO 13395:1997(FIA), respectively. Organic N was calculated as the difference of total N and inorganic N (i.e., the sum of NH_4^+-N and NO_3^--N). Water analyses were carried out at Suomen Ympäristöpalvelu, which is currently part of Eurofins Ahma Oy. The laboratory holds accreditations for all of these methods except the titration of acidity.

The loads of substances for each plot were calculated using the following equation:

$$\text{Annual load}\left(\text{kg ha}^{-1}\right) = C_w \times Q$$

where, C_w is the runoff weighted average concentration (mg l^{-1}) in water samples and Q is the cumulative mean discharge (l ha^{-1}) during the period represented by the water sample.

2.7. Measurements of GHG emissions

To measure GHG emissions, one metal collar (60 cm × 60 cm) was installed permanently into the soil next to each GW pipe, which made four replicates within every six plots. In summer 2017, GHG emissions were measured six times between July 7 and August 30 using the closed chamber technique (Nykänen et al., 1995). The dark chamber (60 cm × 60 cm × 40 cm) was placed on top of the collar, and the groove of the collar was filled with water to make the chamber airtight. During the 30 min closure, four gas samples of 20 ml were taken with a 60 ml plastic syringe and injected immediately into pre-evacuated 12 ml gas vials. The gas samples were analyzed with a gas chromatograph (HP 7890 Series, GC System, Agilent, USA) equipped with flame ionization (FID) and electron capture detectors (ECD) and a nickel catalyst for converting CO_2 to CH_4. The precolumn and analytical columns were 1.8- and 3-m long steel columns packed with Hayesep Q (80/100 mesh). The GC had a 10-way valve with a 2 ml sample loop and a backflush system for flushing the precolumn between the runs. A 6-way valve passed the flow to either the FID or the ECD. The temperatures of the GC oven, FID, and ECD were 70 °C, 300 °C, and 350 °C, respectively. Nitrogen was used as the carrier gas and a mixture of argon and methane (5%) as a make-up gas (1.4 ml min^{-1}) to increase the sensitivity of the

ECD. An autosampler (222 XL Liquid handler, Gilson Medical Electronics, France) fed the samples to the loop of the GC.

2.8. Statistical methods

Quantities of precipitation and discharge were aggregated into monthly values and allocated to the corresponding water samples. Differences in the chemical characteristics of soil layers were tested with one-way ANOVA. Linear correlation coefficients were calculated for the characteristics of the discharge water samples.

Differences of N, P, and TOC concentrations of water samples were tested after grouping the plots into those with a thicker (Plots 1, 2, 4) or thinner (Plots 3, 5, 6) layer of organic material. Another grouping was carried out based on the AS soil characteristics (Plots 1, 3, 5 and 6 vs. Plots 2 and 4). The soil properties of each plot that are the basis for these groupings will be presented in detail in the Results section. Testing of the different concentrations was done by estimating analysis of covariance (ANCOVA) models for the repeated measurements. These models were analyzed in the SAS program's procedure for generalized linear mixed models (GLIMMIX). The version of base SAS was 9.4 and the GLIMMIX procedure that was used in the modelling was from the analytical package SAS/STAT 15.1. Before the actual model building was done, transformations of the model variables were considered by studying the relationships among dependent variables and possible covariates. Either levels or logarithms of the variables were used in the final models. Logarithmic transformation was chosen if it seemed to guarantee a better model due to a statistically more normal relationship between a dependent and an independent variable. Time effects were taken into account by fitting a time trend or period dummies into a model. The applied within-subject covariance structure was selected from several spatial structures by comparing values of information criteria. The spatial covariance structures allow for autocorrelation and can be applied to data that have unequally spaced repeated measurements. Degrees of freedom and standard deviation approximations for the F tests were calculated according to Kenward and Roger (2009).

3. Results

3.1. Carbon and nitrogen contents of the experimental field

The thickness of the horizons rich in soil organic carbon (SOC) varied from 20 to 80 cm (Fig. 1C, D). Plots 1, 2, and 4 had thicker, and plots 3, 5, and 6 thinner, topsoil horizons rich in SOC. This is the basis for the division of the plots into two groups. Below these horizons, there was a sharp decline of SOC to values ≤1% SOC (Fig. 2A, Supplementary Table S2). The subsurface drainage pipes of all plots were thus clearly installed in the mineral soil at least 60 cm below the horizons consisting of organic material. The mineral subsoil underneath the organic material consisted of coarse silt and fine sand, and the mineral material in the topsoil rich in SOC likely also consisted of these particle size fractions, amounting to 42–59% in Plots 1–5 and about 70% in Plot 6. Clay was detected deeper, 0.9 m in Plots 1 and 2, with a gradual and consistent deepening down to 1.9 m in Plot 6. In the study area, the clay fraction is dominated by mica, chlorite, and amorphous material (Fe and Al hydroxides), while the coarser fractions mostly consist of quartz and feldspars (Sippola, 1974).

SOC stocks of each plot and horizon are shown in Supplementary Table S2. Within the uppermost 100 cm of Plots 1, 2, and 4, the SOC stock was 627–666 tons ha^{-1}, while in Plots 3, 5, and 6, the stock was 237–263 tons ha^{-1}. These are rough estimates because the thickness of the organic horizons varied within each plot, but they well illustrate the difference between the two parts of the field.

The total nitrogen (TN) concentration of soil was associated with SOC, and the TN stock (Supplementary Table S2) in Plots 1, 2, and 4 within the top 100 cm of soil ranged from 35 to 39 tons ha^{-1}, while in Plots 3, 5, and 6, it ranged from 14 to 16 tons ha^{-1}. Between 100 and 200 cm, the TN stock in Plots 1–5 was 6–10 tons ha^{-1}, and in Plot 6, it was only 2 tons ha^{-1}.

In spring 2020, before fertilization, there were large differences in the amounts of Nmin between the different soil layers (Supplementary Fig. S2). When studied at 50 cm-intervals, the soil at 50–100 cm was the lowest in Nmin in all plots, while the water-logged soil at 150–200 cm contained at least as much Nmin as the topsoil at 0–50 cm. In all plots, the NO_3^--N stock, concentrating in the surface layers, amounted to only around 14 kg ha^{-1}, because it was depleted by leaching in autumn and spring. The NH_4^+-N stock was much larger at all depths. In Plots 1, 2, and 4, which had a larger TN stock, the amount of NH_4^+-N was as high as 208 kg ha^{-1}, but it was only 62 kg ha^{-1} in Plots 3, 5, and 6.

3.2. Soil pH and readily soluble mineral elements

The measurement of pH throughout the entire soil profile in two locations (drilling P1 at the edge and more centrally located P2 in Fig. 1B) suggests that the subsoil of the whole area had acid sulfate (AS) soil characteristics. The measurements down to 3 m (Fig. 2B) showed that Plot 3 (drilling P1) had a fresh pH of 3.5–3.9 at 0.4–1.0 m, indicative of the thionic horizon. In drilling P2, close to Plot 6, the thionic horizon with a fresh pH 3.7 occurred at 1.0–1.2 m. Based on the pH drop in the incubation test, the soils contained sulfidic material below 1.0–1.2 m. According to the results from GTK (2021), total S concentration between 0.8 and 2.0 m ranged from 0.32% to 1.02% in P1 and from 0.45 to 0.79% in P2, with the maximum occurring at 1.2–1.4 m at both drilling sites.

For the presentation of soil test results (Supplementary Table S3), the plots were divided into two groups based on the AS soil properties (S, pH, EC) because, in terms of other characteristics, the field was more uniform. In Plots 1, 3, 5, and 6, stacked in the north-western part of the field (Fig. 1B), AS characteristics were more clearly pronounced

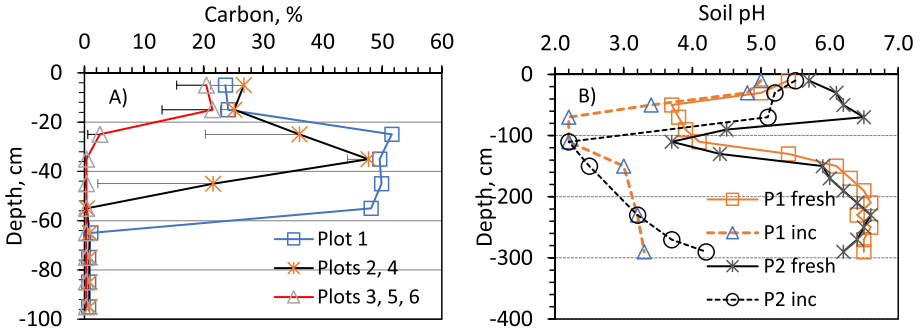

Fig. 2. A) The concentration of soil organic carbon (SOC) in the experimental plots. Plots 3, 5, and 6 represent plots of thinner, and Plots 1, 2, and 4 thicker layers of organic material. The error bars show the standard deviation. B) The pH of soil profiles in Plot 3 (drilling site P1) and close to the edge of Plot 6 (drilling site P2) upon sampling (fresh) and after eight week's incubation (inc). The exact locations of P1 and P2 appear in Fig. 1B. The pH data were retrieved from GTK (2021).

than in Plots 2 and 4 in the south-eastern part of the field. Concentrations of chemical elements are presented in mg l^{-1} of soil, because the material varied in bulk density from 0.15 mg l^{-1} in the horizons richest in SOC to 1.6 kg l^{-1} in the mineral subsoil. As determined in soil testing, regular fertilization and liming had elevated the exchangeable Ca, Mg, and easily soluble P concentrations and the pH of the topsoil. At the depth of 40–80 cm, fresh pH values lower than 5.0 were measured in all plots, with a minimum at 3.7 in Plot 6. At the depth of 80–100 cm, pH values as low as 3.5 were measured in Plots 1 and 6, indicating actively oxidizing sulfidic materials. The lowest fresh pH values were associated with elevated EC and concentrations of easily soluble S. The conversion of measured EC to EC in saturated paste extract, according to Richards (1954), resulted in estimates of 3.2–12.5 dS m^{-1} at the depth of 80–100 cm in the north-western end of Plots 1, 3, 5, and 6, indicating salinity caused by the oxidation of sulfidic material. Soluble S concentration correlated closely ($r = 0.98$, $p < 0.001$) with EC. Where the EC was the highest, soluble S concentration exceeded the threshold value of 500 mg kg^{-1} for a thionic horizon (IUSS Working Group WRB, 2014), with the maximum concentration of 1200 mg kg^{-1} (converted from the soil test result of 1620 mg l^{-1} in Supplementary Table S3 using the bulk density of 1.35 kg dm^3) being found in Plot 1.

3.3. Soil classification

Based on SOC content and the thickness of the organic horizons, Plots 1, 2 and 4, and part of Plot 3, had a histic horizon thick enough (≥40 cm) to qualify as Histosols, while Plot 5 and part of Plot 3 had a thin (10–20 cm) histic horizon. Furthermore, according to the WRB criteria, the topsoil of Plot 6 did not consist of organic material, but had an umbric horizon. The AS soil properties were indicated with Thionic and Sulfidic qualifiers. The organic material was sapric, and artificial drainage justified the drainic qualifier. Classification of the plots according to the WRB system (IUSS Working Group WRB, 2014) was as follows:

1 and 3 (partly): Drainic Sapric Thionic Histosols (Sulfidic)
2 and 4: Drainic Sapric Histosols (Sulfidic)
5 and 3 (partly): Gleyic Histic Umbrisols (Drainic, Thionic, Sulfidic)
6: Gleyic Umbrisols (Drainic, Thionic, Sulfidic).

3.4. Hydrology and soil temperature

In the first hydrological year the precipitation was 544 mm, very close to the average annual for 1981–2010 (541 mm), while the second hydrological year was less rainy (458 mm). The discharge peaked in April–May (max 99 m^3 ha^{-1} day^{-1}) and in autumns (Supplementary Fig. S3), even though in autumn 2018 the discharge remained low (max 4 m^3 ha^{-1} day^{-1}). The monitoring started in October 2016 and weather statistics indicate that the measured discharge peak in November 2016 (25 m^3 ha^{-1} day^{-1}) represented the major outflow period in that autumn; this was hydrologically comparable with the autumn peak in October 2017 (19 m^3 ha^{-1} day^{-1}). In summer periods, there was hardly any discharge from the plots. In the three summer months, the precipitation was 240 mm and only 156 mm in the two hydrological years, respectively, and the potential evaporation in May–August of the second year (386 mm) was much higher than in the first summer (266 mm), resulting in plenty of empty pore space in the soil at the end of the second summer. As a consequence, no water samples could be obtained for almost six months, between early May and late October of the second hydrological year. In the dry (second) year, the mean RR was 41% (range 27–49%), and in the average (first) year it was 46% (31–64%) (Table 1). However, the RR varied among the plots from 27 to 64%, suggesting that Plot 1, in the corner of the field (see Fig. 1B), may have received surface runoff from adjacent Plot 2 in the first year. In the dry year, the RR in Plot 2 was very low, suggesting seepage alongside the main drain. Because the surface runoff among plots could not be measured and the RR calculated from the discharge varied inconsistently among them, the average runoff through the drainage pipes during a given hydrological year was used in the calculation of loads.

Table 1
The amount of precipitation (mm) in each hydrological year, amount of drainage water (D, mm) and the runoff ratio (RR, %) at each plot.

Hydrological year and precipitation	Plot 1		Plot 2		Plot 3		Plot 4		Plot 5		Plot 6	
	D	RR	D	RR	D	RR	D	RR	D	RR	D	RR
1: 544	348	64	171	31	219	40	312	57	226	41	221	41
2: 458	226	49	123	27	214	47	198	43	210	46	143	31

In the present monitoring period of two years, the duration of frost, from late autumn until the beginning of melting, was six months for 2016–2017 and four months and 10 days for 2017–2018 (Supplementary Fig. S3). During the first winter, the frozen soil extended deeper (36 cm) than in the second winter (19 cm). It is noteworthy that half (12) of the discharge water samples (altogether 23) were obtained from soil that was frozen at shallow depths. In 2017, 37–51% of discharge came during the period when the surface soil layers were frozen, and in 2018 the proportion was 26–45%, except for Plot 6, where only 14% of discharge was collected when there was frost in the surface soil layers. According to the long-term (1989–2002) monitoring of soil temperature by the Finnish Meteorological Institute (data not shown), soil temperature at the depth of subsurface drainage pipes varied between 1 and 11 °C within a year and was above 5 °C for five months.

Monitoring of GW level in July–August 2017 (Fig. 3A) showed that, in most plots, the GW level was only slightly below the subsurface drainage pipes, while in Plot 6 the GW level was deeper. The increased GW level at the end of August 2017 in all plots was due to abundant rain (56 mm) during the three last days of the month. During the dry summer of 2018 (Fig. 3B), GW was lower, except in Plot 1, where GW did not decrease below the subsurface drainage system. In Plots 2, 3, 4, and 5, the GW level went below the drainage pipes in early July for about three months and reached a maximum depth of 156 cm in early August. In Plot 6, GW decreased below the GW pipes (200 cm) for more than three months in 2018 and was elevated to only 150 cm by the end of the year, explaining the very small amount of discharge from this plot in autumn 2018.

According to the GW results, we estimated two possible GW flow path patterns, a high and a low GW pattern (see Fig. 1D). During high GW, subsurface drains function efficiently and they dominate the groundwater flow. When GW drops below the subsurface drain pipes, the flow pattern changes and percolation to the large open main drains around the field is supposed to be the primary GW flow pattern.

Regarding conditions conducive to the oxidation of sulfidic material and the production of acidity and sulfate in the drainage water, at least the upper parts of the sulfidic horizons were above the GW level in 2017, with the possible exception of Plot 1. During a severe drought in 2018, GW dropped so low that sulfidic materials were no longer water-saturated in Plots 2–6. Deep GW likely allowed the sulfidic subsoil to be oxidized in Plots 2–6. According to GW results we estimated two possible groundwater flow path patterns, a high ground water pattern and a low groundwater pattern (see Fig. 1D). During the high GW subsurface drains function efficiently and they dominate groundwater flow pattern. However, when GW drops below subsurface drain pipes the flow pattern changes and percolation to deeper main drains is supposed to be the primary GW flow pattern. It should be noted that our preliminary estimation must be verified for example by stable water isotopes in further studies.

3.5. Characteristics of water samples

The concentrations of TOC and N in discharge water and the amounts that were leached differed from plots with large SOC stock (1, 2, 4) and small SOC stock (3, 5, 6) (Supplementary Table S4). The differences were statistically significant for TOC, total N (TN), and organic

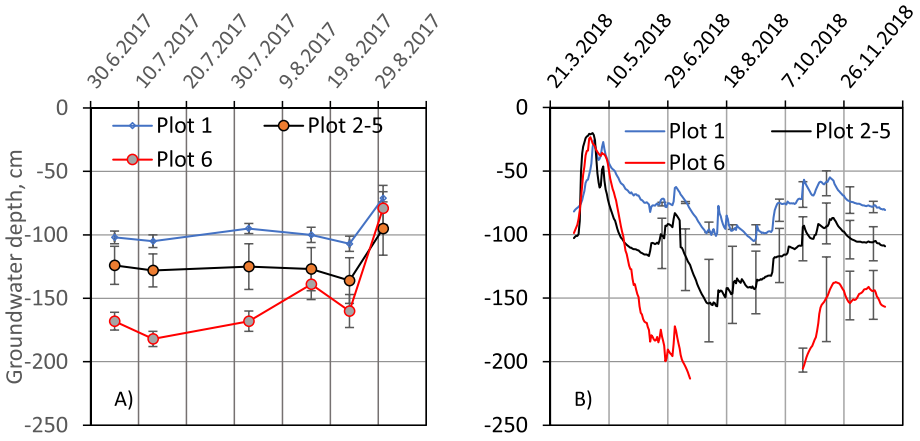

Fig. 3. The groundwater level in the experimental plots in A) July and August 2017 (manual measurements) and B) March through December 2018 (logger data). The error bars in A) stand for ±standard deviation on each measuring day in 2017 and 10-day intervals in 2018. Where the error bars are not presented, the results are based on data from one logger only.

N (Norg), as confirmed by ANCOVA tests. The TOC concentration (Supplementary Fig. S4) peaked at the beginning of the high flow period in the autumn, and the minimum values with little difference between the two groups of plots were reached during the most intensive discharge, in the spring. Altogether, 190 kg of TOC ha^{-1} leached from Plots 1, 2, and 4, while only 94 kg ha^{-1} leached from Plots 3, 5, and 6.

The discharge from the plots with a larger SOC stock (1, 2, 4) had substantially higher TN concentrations compared to Plots 3, 5, and 6 (Fig. 4A–B). The highest TN concentrations were measured during the high flow period, in spring 2017, and the lowest concentrations during low discharge. The fluctuation in TN concentration was mostly caused by NO_3^--N, and the peak values of TN predominantly consisted of

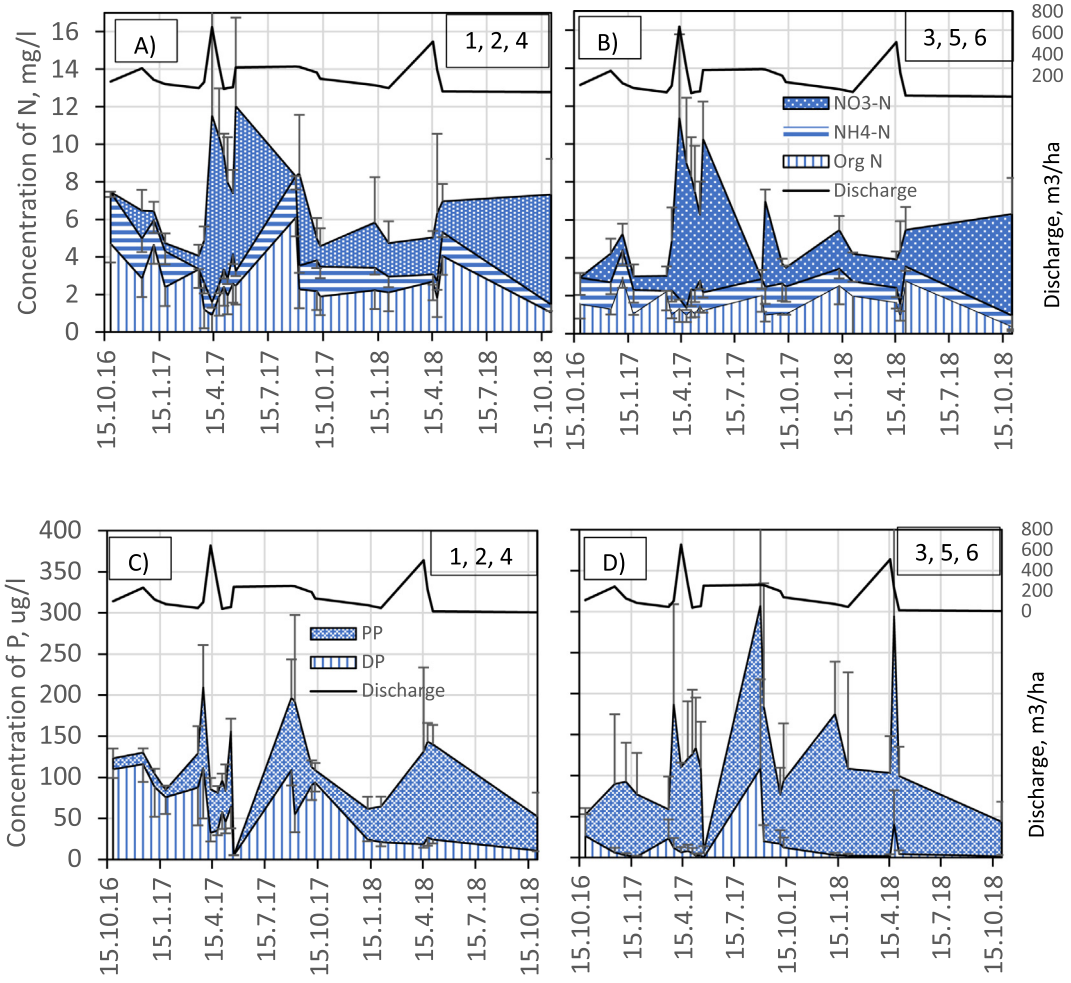

Fig. 4. The concentrations of different N (A–B) and P (C–D) fractions in the discharge and the average monthly amounts of discharge. PP = Particulate phosphorus, DP = Dissolved phosphorus.

NO_3^--N. For example, in April–May 2017, during the abundant discharge, about 70% of TN consisted of NO_3^--N while in the winter months of 2017, only about 20% of TN in the discharge consisted of NO_3^--N. The flow-weighted average NO_3^--N concentration of individual Plots was at 1.1–4.8 mg l^{-1}, and no values above 10 mg l^{-1} were measured. Among the plots with thicker organic layers, Plots 1 and 2 produced water with higher NO_3^--N concentrations (3.0 and 4.7 mg l^{-1}) than Plot 4 (2.0 mg l^{-1}). The concentrations of Norg or NH_4^+-N were much more stable within the two groups of plots than those of NO_3^--N. Norg concentration correlated with TOC ($r = 0.67$, $p < 0.001$).

The proportions of NO_3^--N, NH_4^+-N and organic N for the entire monitoring period were 41, 23, and 36%, respectively. It is noteworthy that the proportion of NH_4^+-N of TN was highest in the water samples of Plot 6 (40%) and those peaks coincided with the lowest pH in water ($r = -0.66$, $p = 0.0011$), while in the whole material this correlation was non-significant.

The average TN load in the rainier hydrological year was 19.6 kg ha^{-1}, from Plots 1, 2, and 4, with a high SOC stock, and 10.9 kg ha^{-1}, from Plots 3, 5, and 6 with a smaller SOC stock. In the drier hydrological year, the TN loads were smaller than in the rainier year but again higher from plots with a high SOC stock (Supplementary Table S4).

We are aware that during this monitoring period surface runoff was not collected comprehensively; therefore, the loads calculated based on the discharge alone are underestimates. We have preliminary results of runoff volumes for the year 2020, when the surface runoff was properly collected. In that year, surface runoff represented 30% of the total drainage of the plot next to the surface runoff collector. During the monitoring period, we could obtain two surface runoff samples. Assuming those concentrations are representative, we can calculate that during the monitoring period loads of different substances through the subsurface pipes represented 83% of total N and 88% of TOC loads.

The flow-weighted mean total P (TP) concentration of discharge from different plots ranged between 98 and 170 μg l^{-1} (Fig. 4C–D), with no consistent connection to soil properties. Instead, dissolved P (DP) was higher (51–74 μg l^{-1}) in Plots 1, 2, and 4, which had a larger SOC stock compared to 12–32 μg l^{-1} in Plots 3, 5, and 6, while particulate P concentration behaved in the opposite manner. When calculated for the entire monitoring period, the proportion of DP was 49–54% in plots rich in SOC, while only 12–22% was in dissolved form in the waters of Plots 3, 5, and 6 ($F = 101.9$, $p < 0.001$). There was a tendency of high TP and DP concentrations during the peak discharge periods, with decreasing concentrations toward the end of the high flow. The higher proportion of DP in Plots 1, 2, and 4, compared to the rest of the plots, seems to be associated with the different thicknesses of organic materials in the two groups of plots and not to tillage operations. In particular, no tillage was applied to Plots 1 and 2 in autumn 2016, while Plot 4 was ploughed, but the three plots had similar proportions of DP in all discharge samples until spring 2017. According to the ANCOVA tests, the difference between the plot groups was statistically significant for DP, but insignificant for TP.

The annual TP load in the first hydrological year ranged from 0.17 to 0.50 kg ha^{-1} (Supplementary Table S5) Even though the highest load came from Plot 1, which had the thickest layer of organic material, the load was dependent on the amount of discharge and there was no consistent relationship between the SOC stock of a given plot and the TP load ($r = -0.227$, $p = 0.665$). In the second hydrological year, the range of TP load was 0.13–0.37 kg ha^{-1}. The dissolved P load in the entire monitoring period was highest (0.43 and 0.26 kg ha^{-1}) from Plots 1 and 4, which had the thickest horizons of organic material, while 0.05–0.17 kg ha^{-1} were leached from the other plots. In the same manner, as for N, we can roughly estimate that TP in drain discharge represented 64% of TP and 68% of DP load.

3.6. Characteristics related to acid sulfate soil

Despite the firm evidence of the AS subsoil in all plots, the pH of the discharge water from Plots 1, 2, 4, and 5 was above 6.0 throughout the experimental period and above 5.0 in water samples from Plot 5, except for one sample (Fig. 5A), suggesting that the sulfidic horizons were oxidizing only to a moderate extent due to the rather high GW levels in most of the plots. In Plot 6, the discharge water exhibited pH 3.8 in autumn 2017, and the pH values were just above 4.0 in the springs of 2017 and 2018. It is noteworthy that this plot also often produced discharge that had a pH of more than 6, particularly at the beginning of the high flow periods. Plot 3 also occasionally produced discharge of pH <5.5. More clearly than by pH, the plots differed by a load of titratable acidity. While Plots 2 and 5 yielded only 1400 mol ha^{-1} acidity during the entire monitoring period, the other four plots (1, 3, 4, 6) yielded 2300–2800 mol ha^{-1}. Electrical conductivity, reflecting the concentration of charged solutes in the discharge, ranged from 30 to 110 mS m^{-1}, which, according to

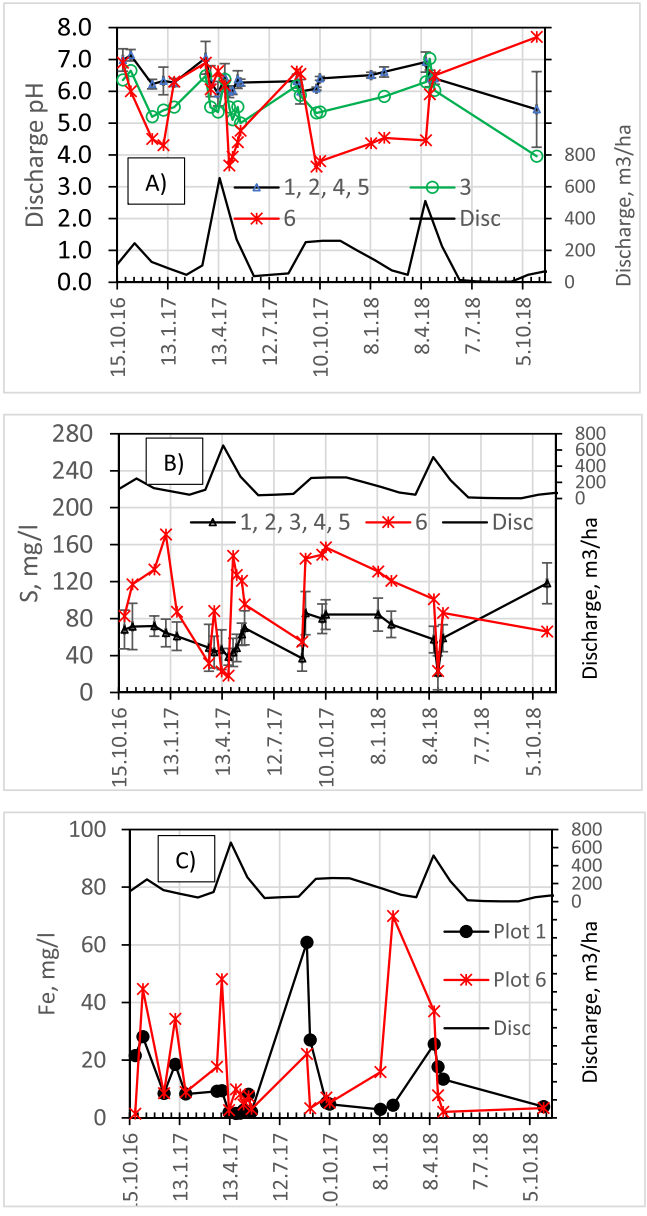

Fig. 5. A) The pH, B) sulfur concentration, and C) Fe concentration of the discharge water. The average amount of the monthly discharge is expressed in all figures. The error bars in A) and B) express the standard deviation.

the equation presented by Griffin and Jurinak (1973), correspond to the ionic strength of 0.004–0.015 mol l^{-1}. The highest values in the water samples of all plots occurred in autumn 2017, and the lowest values were in April–May, when snowmelt water diluted the discharge.

The overall mean flow-weighted S concentration of the water samples was 71 mg l^{-1}, while the corresponding results of individual plots ranged from 46 (Plot 4) to 106 mg l^{-1} (Plot 6). In all the other plots (1, 2, 3, 5), S concentrations were within a narrow range of 62–76 mg l^{-1}. The concentration of S was smallest at the beginning of the snowmelt or rainy periods (Fig. 5B), but the concentration increased over time when the high flow continued. There was a strong positive correlation ($r = 0.898$, $p < 0.001$) between the S concentration of the discharge water and EC, but a moderate negative correlation ($r = -0.61$, $p < 0.001$) with pH. Plots 1 and 6 produced the highest S loads, altogether 449 and 394 kg ha^{-1} during the monitoring period, owing to the high discharge (Plot 1) and high S concentration in the water (Plot 6). Plots 2 and 4 produced the lowest S load (232 and 246 kg ha^{-1}), in accordance to the easily soluble S in the soil (Supplementary Table S3).

The concentrations of Al correlated with the discharge water pH ($r = -0.645$, $p < 0.001$). The highest Al concentrations were measured in water from Plot 6, which was associated with the discharge of the lowest pH values. In the other plots, Al concentrations were rather stable and low, with the median values of these four plots being only 0.6–1.4 mg l^{-1} (Supplementary Table S6). As for Fe, there was a strong fluctuation of the concentration in every plot, and it was common during high flow periods for there to be sudden increases or decreases of Fe concentration within one week (Fig. 5C); the peaks were observed sporadically in different plots. The peak concentrations commonly occurred at the beginning of the high flow and decreased rapidly. Contrary to Al, there was no negative correlation between the discharge Fe concentration and pH ($r = 0.008$, $p = 0.926$), and the highest Fe concentrations commonly occurred in water samples that had a pH around 6, not in the most acidic water samples. The Fe load was about 8-fold compared to Al. Even though the highest Fe loads were produced from Plots 1 and 4 (which had thicker layers of organic material) and the smaller loads came from Plots 3, 5, and 6 (which had thinner layers of organic material), Plot 2, with a thick cover of organic material, produced the smallest load in both hydrological years.

3.7. Greenhouse gas emissions

During the eight-week monitoring in July and August 2017, CO_2 emissions were highest in the beginning of August for all study plots (Fig. 6A). Toward the end of August and the growing season, the CO_2 emissions decreased similarly in all plots. There was a trend that the highest CO_2 emissions occurred from Plots 1 and 3, and the lowest emissions were from Plots 5 and 6, but the difference was not statistically significant. The average amount of CO_2 emitted for the whole eight-week measurement campaign for Plots 1, 2, and 4 was 120 ± 53 kg CO_2-C ha^{-1} d^{-1}, while for Plots 3, 5, and 6, it was 117 ± 40 kg CO_2-C ha^{-1} d^{-1}, respectively. Nitrous oxide fluxes were highest in early July, when the measurement period for GHGs started (Fig. 6B). On the third measurement day, August 2, 2017, the N_2O fluxes were slightly increased in some study plots. Thereafter, N_2O fluxes decreased similarly in all plots toward the end of August. Like the CO_2 emissions, N_2O fluxes seemed to be the smallest in Plots 5 and 6 and highest in Plots 3 and 4, but there was no statistical significance. The average N_2O emission for the whole measurement campaign for Plots 1, 2, and 4 was 49 ± 68 g N_2O-N ha^{-1} d^{-1} and for Plots 3, 5 and 6 it was 29 ± 46 g N_2O-N ha^{-1} d^{-1}, respectively. CH_4 uptake was usually measured in all study plots. In some cases, a small flux was measured, but on average the CH_4 fluxes were close to zero (Fig. 6C). For Plots 1, 2, and 4, the average CH_4 emission for the whole measurement period was −2.4 ± 4.4 g CH_4-C ha^{-1} d^{-1}, while for Plots 3, 5, and 6, it was 0.8 ± 4.0 g CH_4-C ha^{-1} d^{-1}.

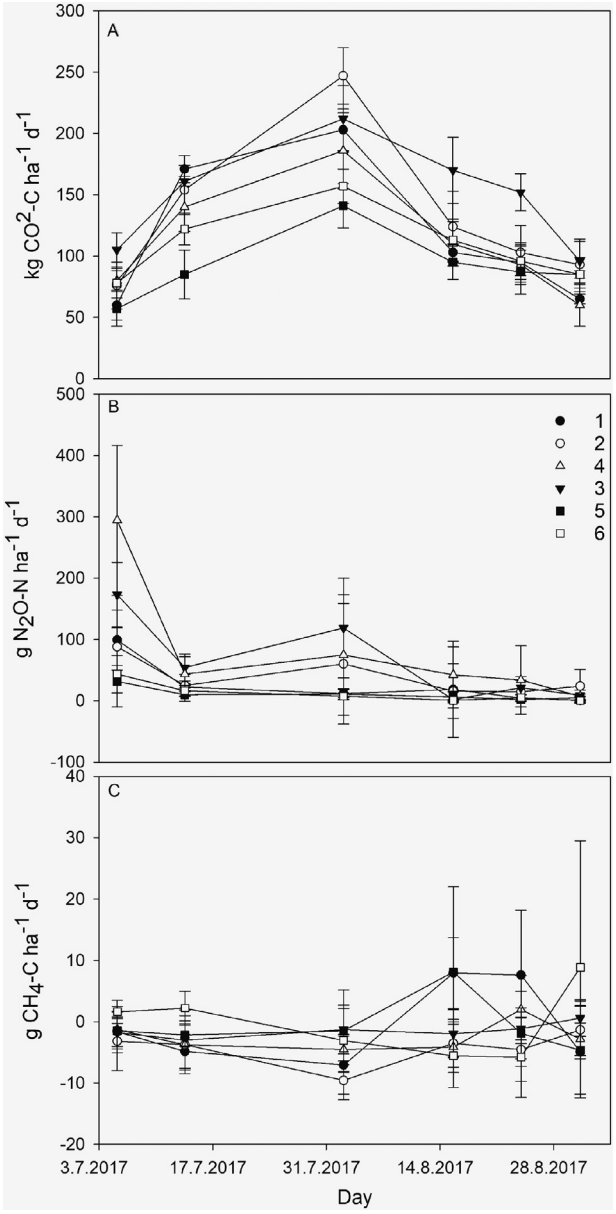

Fig. 6. A) Carbon dioxide, B) nitrous oxide, and C) methane fluxes from the different study plots of the cultivated peatland at the Ruukki research station. Carbon dioxide results are represented as kg CO_2-C ha^{-1} d^{-1} and nitrous oxide and methane results as g N_2O-N ha^{-1} d^{-1} and g CH_4-C ha^{-1} d^{-1}. Error bars represent standard deviation ($n = 4$). In Plots 1, 2, and 4, the peat depth is approximately 70 cm, and in Plots 3, 5, and 6, it is between 15 and 30 cm.

During the period when GHG fluxes were measured, the GW level ranged between 70 and 175 cm below the soil surface (Fig. 3A). The GW levels were, on average, deepest when the GHG flux measurements started at the beginning of July 2017 and when the growing season was most active. At the end of August, the GW level was increased closer to the soil surface, and CO_2 and N_2O fluxes decreased simultaneously. The GW level did not affect CH_4 fluxes. The CO_2 fluxes were smallest when the GW level was less than 60 cm from the soil surface and highest when GW was between 70 and 130 cm. Further, the N_2O fluxes were highest when GW was between 70 and 130 cm. Outside this range, the N_2O fluxes were rather small.

4. Discussion

4.1. Substantial differences in soil properties among the study plots

Our 19.6-ha experimental field contains substantial heterogeneity, in spite of its flat and uniform appearance from the soil surface. The major factors of heterogeneity among the six plots include 1) thickness of the horizons consisting of organic material, 2) uneven manifestation of acid sulfate (AS) soil characteristics, and 3) hydrological differences exhibited by different amounts of drainage flow. This spatial variability has impacts on environmental loading from different parts of this field. The thickness of organic material varies notably and is reflected in soil classification. Plots 1, 2, and 4 are Histosols, and Plots 5 and 6 are mineral soils with histic or umbric topsoil, while Plot 3 is partly Histosol and partly Umbrisol with a thin (<40 cm) histic horizon. The plots with a thicker peat layer (1, 2, 4) may have been natively wetter, partly attributable to the clayey subsoil closer (0.9 m) to the soil surface than in the rest of the plots (1.9 m); this has been conducive to the decreased decomposition of organic matter. The thickness of the organic material may also reflect the agricultural drainage history, because the plots that have an older subsurface drainage are characterized by a thinner peat layer. Several studies (e.g., Maljanen et al., 2007) reported large CO_2 emissions from cultivated organic soils, which gradually results in a marked loss of SOM and a thinner, or even disappearing, peat layer. In Plot 6 which was subsurface drained in the early 1900s, the peat layer of unknown original thickness has practically disappeared, but Plots 1 and 2, which were subsurface drained for the first time in the 1980s still have 60–80 cm of peat. The division of plots based on the thickness of organic material comprises an experimental factor associated with the topsoil. As for the subsoil, all plots contained sulfidic material, but its effect on drainage water quality varied temporarily and from plot to plot. Since uniform water management was applied to all plots, variable drainage flow and GW levels indicated native hydrological differences among the plots. The abundant stock of SOM above the drainage pipes constitutes a release potential of dissolved organic C and mineral N that is enhanced by wetting and drying cycles. Furthermore, when GW is low, sulfidic material at and below the drainage pipes can oxidize to sulfate (SO_4^{2-}), oxyhydroxysulfates, and ferrihydrite. Environmental loading from this field is impacted both by histic and AS characteristics, and the results must not be interpreted as an effect of either of these characteristics alone.

Soil temperature, moisture, acidity, the availability of decomposable organic matter, and redox conditions have an impact on biological, chemical and transport processes taking place in the soil. In our experiment, half ($n = 12$) of the drainage water samples ($n = 23$) were taken during periods when the topsoil was frozen. However, soil temperatures below 50 cm are above 0 °C throughout the year, enabling wintry drain discharge, which reflects the pore water characteristics of the subsoil. A summer mean soil temperature of 12.8 °C was measured at 20 cm depth between 1976 and 1990 at the Ruukki site (Heikinheimo and Fougstedt, 1992), indicating favorable conditions for aerobic microbial activity in the summer, in spite of occasional droughts that may impede biological activity. The mean summer soil temperature decreases with depth, settling at 9.2 °C at the depth of the drainage pipes and 5.7 °C at 200 cm (Heikinheimo and Fougstedt, 1992). This slows down, but does not stop, chemical and microbiological reactions. Water saturation hinders aerobic reactions, but promotes reducing reactions, in large parts of the subsoil most of the year. The low pH (<4) of the thionic subsoil horizons caused by the oxidation of sulfidic material also decreases the biological activity of subsoil horizons in AS soils (Šimek et al., 2011). Furthermore, the low concentration of organic matter in the entire mineral subsoil likely limits the activity of heterotrophic microbiota. In summer, reaction products are accumulated and not transported out of the soil because of the lack of discharge. In autumn and spring, rain or melting water fills the pores and carries dissolved substances to the drainage pipes. Sulfate is probably transported first, followed by Fe as soon as ferrihydrite has dissolved during anaerobic periods. The transport of Fe can also be enhanced by complexation with organic matter in pore water. Thus, the loads are dependent on the production rate of soluble substances and the effectiveness of the transport processes, both of which are spatially and temporally variable.

4.2. Differences in nitrogen fractions of discharge water among soil types

The proportions of N fractions in the discharge water in Ruukki differed from those of mineral soils. In the Ruukki field, Norg comprised a substantial part (two-year average of different plots 33–44%) of TN, and there was no systematic difference in the species distribution between the plots of small or large soil SOM stock. In turn, the proportion of NO_3^--N was only 30–52%, while NO_3^--N commonly dominates in the discharge of mineral soils, comprising 94% of TN from a mineral acid sulfate soil in 2011–2017 (Yli-Halla et al., 2020), 85% from a clay soil in Finland in 1991–1993 (Turtola and Paajanen, 1995), and 78% from a 449-ha catchment dominated by cereal cropping in south-eastern Norway (Chen and Bechmann, 2019). The proportion of NH_4^+-N (12–24% at Plots 1–5) was substantially higher than in mineral soils. In that respect, our shallow peat soil is similar to the 3–4 m-thick peat soil of Huhta and Jaakkola (1993), where NH_4^+-N comprised 5–16% of TN in the discharge. In our study, the NH_4^+-N proportion in Plot 6 (37%) represented an even larger share (37%) than NO_3^--N, although the NH_4^+-N stock was not the most abundant at this plot. Simultaneous peaks of low pH and high NH_4^+-N concentrations at this plot suggest that the peaks were associated with the transport of solutes from deeper horizons where sulfidic material had been oxidized and that nitrification had been prevented by acidity or anoxia. The high proportion of NH_4^+-N in the discharge water from Plot 6 may also be explained by the reduction of NO_3^--N to NH_4^+-N coupled with the oxidation of sulfides in the actively oxidizing AS soil layer (Brunet and Garcia-Gil, 1996). An abundance of NH_4^+-N seems to be typical of peat soils, as reported in the discharge waters of several peat mining areas in Finland (Heikkinen et al., 2018). These results show that, in peat soils, the determination of NO_3^--N alone is not sufficient when estimating N leaching, but TN needs to be explicitly measured.

4.3. Soil properties influence nitrogen and carbon concentrations in discharge waters

A major observation from our field was that the thicker the layer of organic material and larger the SOC stock, the higher the TOC and TN concentrations were in the subsurface drainage waters. However, the leaching of TOC and TN seem to have rather different temporal patterns. TOC concentration peaked after dry periods at the beginning of the high flow in autumns 2016 and 2017. It is likely that the previous dry periods promoted SOM transport, since air drying substantially increases the water solubility of SOM (Kaiser et al., 2015, with references). In autumn, the leaching of TN occurred slightly later during the runoff peaks, suggesting that a major part of the N originates from the interiors of soil aggregates, from where N slowly diffuses into macropores in a rewetted soil. Furthermore, TOC concentrations were low during the peak flow in spring, while N concentrations, particularly in the form of NO_3^--N, were high in these water samples. More abundant leaching from Plots 1, 2, and 4 can be partly explained by the mineralization of the large TN stock in soil. These same plots contained a higher Nmin stock, both in the surface layers and in the sulfidic subsoil, likely contributing to the discharge of N as well. The higher NO_3^--N concentrations in Plots 1 and 2 may also be partly attributed to the soil disturbance caused by the extensive ditching activities recently carried out in these two plots.

According to the results compiled in Table 2, the TOC concentrations from all plots were higher compared to agricultural mineral soils (Manninen et al., 2018), where the maximum concentrations (25–30 mg l^{-1}) were similar to the median in our field. Instead, the TOC range in our water samples was similar to that of runoff waters

Table 2
Results of TOC, N, and P concentrations and annual loads in subsurface discharge water compiled from various studies. TOC = total organic carbon, TN = total nitrogen, TP = total phosphorus, DP = dissolved phosphorus.

Reference	TOC mg l^{-1}	TN mg l^{-1}	NO_3^--N mg l^{-1}	NH_4-N mg l^{-1}	TN kg ha^{-1}	TP mg l^{-1}	DP mg l^{-1}	TP kg ha^{-1}	Soil, crop and average annual discharge (mm)
This study	21.7	4.2	1.5	1.3	9.3	0.13	0.022	0.29	0.2–0.3 m peat, 218 mm
	43.5	7.1	3.4	1.1	15.4	0.12	0.059	0.26	0.6 m peat, 218 mm
Huhta and Jaakkola, 1993	n.d.	8.5	n.d.	0.6	38.2	0.31	0.19	1.4	3–4 m peat, barley hay; 429 mm, 1983–87
	n.d.	4.8	n.d.	0.7	19.1	0.43	0.24	1.7	
Kløve et al., 2010[b]	20.8	2.8	1.2	0.24	21.7	0.30	0.229	2.32	0.6 m peat, 763 mm, perennial grass, 2003–04
Yli-Halla et al., 2020	n.d.	21.1	19.8	0.15	63	n.d.	n.d.	n.d.	Silty clay loam AS soil, 298 mm, cereals, 2011–17
Jaakkola, 1984	n.d.	n.d.	9.0	n.d.	13[d]	n.d.	n.d.	n.d.	Clay, 145 mm, cereals, 1976–82
Turtola and Paajanen, 1995[a]	10.3[e]	7.9	6.8	n.d.	16.4	0.20	0.028	0.59	Clay, 328 mm, cereals, 1991–93
	n.d.	6.2	5.2	n.d.	n.d.	0.23	0.027	n.d.	Clay, 159 mm, ley, 1991–93
Manninen et al., 2018[c]	15.2	n.d.	n.d.	n.d.	n.d.	n.d.	n.d.	n.d.	Fine sand, cereals, mineral fertilization, 2012–14

[a] Period after improved subsurface drainage.
[b] Plot drained with subsurface pipes. Loads during a period of 13 mo 12 d.
[c] Site Toholampi.
[d] NO_3^--N load.
[e] Data of the same field by Manninen et al. (2018) for two years (March 2012–March 2014).

from five peat extraction areas in central Finland (18–81 mg l^{-1}, Heiderscheidt, 2016). Accordingly, the TOC load from our field was higher than (plots of thicker organic horizons) or similar to (plots of thin organic horizons) the loads from mineral soils (25–52 kg ha^{-1}, Manninen et al., 2018), but lower than from a peat soil in Norway (Kløve et al., 2010) where a high TOC load of 159 kg ha^{-1}, despite a similar or lower TOC concentration, can be explained by a 3.5-times higher discharge than in our field.

The discharge from a 3–4 m thick peat soil grown for barley (Huhta and Jaakkola, 1993) had a somewhat similar TN concentration as the waters from our experimental field's 0.6 m peat layer, but the higher discharge from their field was conducive to the higher load. Despite a much lower N concentration in the discharge from a Norwegian peat soil (Kløve et al., 2010), a higher TN load was also measured there because of the abundant amount of discharge. There was no systematic difference in TN concentration in the discharge water between our peat soil and a heavy clay soil from southern Finland (Turtola and Paajanen, 1995). Indeed, our findings suggest that TN leaching from the present shallow peat field was at the same level as or slightly lower than that from mineral soils (15.5 kg ha^{-1}, Tattari et al., 2017; 10–17 kg ha^{-1}, Turtola and Paajanen, 1995). Nitrogen leaching from our experimental field was also much less than that from a mineral acid sulfate soil in Finland, where the TN concentration in discharge water was three- to five-times higher and 50–63 kg N ha^{-1} was annually leached in 2011–2017 (Yli-Halla et al., 2020), even though both fields had a large stock of Nmin in soil horizons below the subsurface drainage pipes. As for the crop, Huhta and Jaakkola (1993) reported in their thick peat soil that TN leaching from perennial hay was only about half of that measured from spring barley plots, suggesting a strong positive influence of a permanent soil cover crop that catches the Nmin that is mineralized. Even though we also grew spring cereals and grass in our field, the experimental set-up and the short duration of the monitoring do not allow us to make conclusions about the effects of different crops on N leaching. A compilation of results thus shows that even though organic soils have a large N stock, it is not always reflected as an abundant N loading, but the concentration in discharge water and the load from peat soil can be at the same level as, or even lower than, that found in mineral soils.

4.4. Phosphorus leaching was controlled by mineral soil contact

The flow-weighted mean TP concentration (0.10–0.16 mg l^{-1}) was quite similar in all plots, but there was a tendency for Plots 1, 2, and 4, of high SOC stock, to produce drainage water with a higher percentage of DP (49–57%) than Plots 3, 5, and 6 (12–23%). Even a higher proportion of DP (50–80% of TP) has been found in a 3–4 m thick peat soil where the drainage pipes were in the peat layer (Huhta and Jaakkola, 1993). While in our field 0.17–0.34 kg TP ha^{-1} were leached annually through the subsurface drainage pipes, 1.3–2.0 kg TP were leached in the experiment by Huhta and Jaakkola (1993). Our results are comparable to those measured in mineral soils, e.g., 0.59 kg ha^{-1} by Turtola and Paajanen (1995). Compared to the average TP load of 1.1 kg ha^{-1}, including surface runoff and discharge, from agricultural land in Finland (Tattari et al., 2017), the present field seems not to be a source area of large P loading. Even taking into account that our results do not include surface runoff and may represent only about 64% of the total P load from the field, an estimate of 0.27–0.53 kg ha^{-1} for the total annual TP load is quite low.

In the Ruukki field, subsurface drainage pipes have been installed in the mineral soil, which likely has a high P sorption capacity, while in the study by Huhta and Jaakkola (1993) the drainage pipes were in the peat layer. Saarela (2008) demonstrated that the risk of P leaching is much higher in soil that has a peaty subsoil compared to mineral soil, even with a peaty plough layer. When evaluating the P loading risk of agricultural peatlands, there is a need to separate shallow peat soils with mineral subsoils from thick peat soils. Our results confirm that the abundance of organic material contributes to a higher DP load, increasing the eutrophication effect of a unit of TP that is transported to watercourses.

4.5. Acid sulfate subsoil causes a risk of acid discharge water

Our experimental field contains a thionic horizon and sulfidic material starting just below the subsurface drain pipes at a depth of 1.0–1.2 m. The oxidation of sulfide, occurring in summer when the GW is low, is indicated by a high SO_4^{2-}-S concentration. However, low SO_4^{2-}-S concentrations were observed at the very beginning of discharge peaks due to rain or snowmelt water, but after the oxidation products had dissolved and diffused from the interiors of soil aggregates into the macropores and further into the drainage system, high concentrations of SO_4^{2-}-S were measured. The strongest peaks of pH and SO_4^{2-}-S, measured in Plot 6, can be attributed to the remarkable lowering of GW in this plot compared to the others, allowing effective oxidation of sulfidic material. The lack of a peak in autumn 2018 in Plot 6 is explained by the hydrological conditions. In October 2018, GW levels were still low after the exceptional drought, and the meager amount of water entering the drain pipes likely represented rainwater from above and not the horizons where sulfide had actively oxidized in summer. Therefore, it was likely that plenty of SO_4^{2-}-S and acidity would leach in the following spring, or whenever the GW level reached the drainage pipes.

In all plots, SO_4^{2-}-S concentrations (median 65 mg l^{-1}) were much higher than commonly measured in non-AS soils (5 mg l^{-1}, Turtola and Jaakkola, 1986). However, the SO_4^{2-}-S concentrations of water samples were much lower than measured in the discharge water of two mineral AS fields in Ilmajoki and Mustasaari about 300 km south,

where the average concentrations were 441 and 2312 mg l^{-1} in five- and three-year monitoring (Bärlund et al., 2004). Accordingly, the average S load (166 and 127 kg ha^{-1} in the two hydrological years) was much lower than in an AS soil in Rintala, about 300 km south of Ruukki (630 kg ha^{-1}, Österholm and Åström, 2004); however, these were almost 10 times higher than is commonly measured in clayey non-sulfidic soils (15–20 kg ha^{-1}, Turtola and Jaakkola, 1986; Eriksen and Askegaard, 2000). Despite a similar total S concentration as in the AS soils mentioned above, Plots 1, 2, 4, and 5 in this AS field did not produce severe loading of acidity, and the discharge water from these plots had a pH of 6.0 or above during this monitoring period. Titratable acidity (median 0.4 mmol l^{-1}) and dissolved Al concentration (median 0.9 mg l^{-1}) were low, when compared to Ilmajoki and Mustasaari (mean for acidity 3.9 and 11.0 mmol l^{-1} and Al 20 and 88 mg l^{-1}, respectively), and the mean pH of discharge waters at those sites were as low as 4.3 and 3.7. The moderate loading of acidity and sulfur, despite a thionic horizon and sulfidic material, may be associated with the protective peat coverage. The peat layer above the mineral soil horizons may consume most of the oxygen via biological decomposition and so inhibit the oxidation of sulfidic material, as reported in AS soils in Australia (Cook et al., 2004). In addition, higher pH values can be explained by the high TOC concentration of drain discharge water, which favors formation of organo-Fe complexes (Herzog et al., 2020) and the co-precipitation of organo-Fe aggregates (Ingri et al., 2018) instead of the precipitation of ferrihydrite with a concomitant release of acidity. This explanation is in agreement with the high dissolved Fe concentrations (median 7.7 mg l^{-1}) compared to mineral AS soils in Ilmajoki and Mustasaari (mean 0.9 and 3.7 mg l^{-1}, respectively). The sporadically peaking Fe concentrations occurring at the beginning of high flow periods may refer to the flushing of rust precipitates from the drainage pipes by high velocity runoff after a stagnant period. Furthermore, the highest Fe concentrations (40–100 mg l^{-1}) in our field were associated with pH values around 6, suggesting that those waters may have originated from the reduced soil layers and not from the acidified aerobic layers, because the most acidic water samples usually had low dissolved Fe concentrations.

4.6. GHG emissions from the Ruukki experimental plots

There were no significant differences in GHG emissions among the study plots. The measurement period for GHG emissions was only eight weeks, extending from the beginning of July to the end of August 2017, and it did not contain fertilization events. The aim of the GHG measurements was to get rough estimates for emissions after establishing the site and to see if there were differences among the plots. In 2017, spring barley was grown in Plots 1–4, and triticale in Plots 5–6. Both crops had received the same fertilization in May. In the study by Yli-Halla et al. (2017), conducted in boreal AS soils, N_2O emissions were higher in sites with 30 cm peat depth, compared to sites with 60 cm peat depth. At the Ruukki site, the GHG emissions were slightly smaller in Plots 5 and 6, with the thinnest peat compared to other sites but without statistical significance. When comparing the average fluxes for Plots 1, 2, and 4 (thicker peat) with those from Plots 3, 5, and 6 (thinner peat), the differences were within the standard deviation.

Since the measurement period did not cover even one whole growing season, and because the most active growing phase earlier in summer (Lohila et al., 2003) was not captured by the measurements, annual emissions cannot be calculated, but the results can be compared to studies that have measured summer time fluxes. Furthermore, recent soil disturbances, from establishing the study field, most likely affected GHG dynamics by producing higher emissions, because more air was introduced to the peat profile than in normal agricultural practices. In our study, the CO_2 fluxes were between approximately 50 and 250 kg CO_2-C ha^{-1} d^{-1}. These are of the same magnitude or slightly higher than in other studies on organic soils. In the study by Lohila et al. (2003), the total ecosystem respiration on barley and grass plots was between 45 and 210 kg CO_2-C ha^{-1} d^{-1} and 45–260 kg CO_2-C ha^{-1} d^{-1}, respectively. In the same study, the total ecosystem respiration for sandy and clay soil growing barley or grass ranged between approximately 10 and 165 kg CO_2-C ha^{-1} d^{-1}. In the study by Nykänen et al. (1995), CO_2 emissions were between 10 and 110 kg CO_2-C ha^{-1} d^{-1} in a peat plot with grass cultivation. The N_2O fluxes were also in the same range as reported in other studies. The N_2O fluxes on grass plots in cultivated peat soil have been between zero and approximately 100 g N_2O-N ha^{-1} d^{-1} and from barley plots between close to 0 and 200 g N_2O-N ha^{-1} d^{-1} with few higher occasions (Regina et al., 2004), whereas in our study the N_2O fluxes from Plots 1–4 growing barley were between close to 0 and 150 g N_2O-N ha^{-1} d^{-1} with few higher fluxes in the first measurement day. In the study by Syväsalo et al. (2006), N_2O fluxes of grass and cereal on sandy soil ranged between approximately 0 and 20 g N_2O-N ha^{-1} d^{-1} under grass cultivation and 0 and 50 g N_2O-N ha^{-1} d^{-1} under cereal cultivation. This study field has been effectively drained and, due to low GW levels, the CH_4 fluxes are usually negative or close to zero (Regina et al., 2007), as was the case in our study.

Methane fluxes were small in all plots, with a range of approximately −10 and +10 g CH_4-C ha^{-1} d^{-1} with quite large variation. Because the research field is well-drained and peat is aerated from the surface, the CH_4 emissions are naturally small compared to pristine peatlands. There were no systematic differences among plots when it came to CH_4 fluxes, but there were indications that, on some days, CH_4 fluxes were highest in Plots 5 and 6 (thin peat). However, CH_4 fluxes in all plots were so small that they had a negligible effect on the overall GHG budget of the research field.

5. Conclusions

In this paper, we introduce a 19.6-ha experimental field that was established in 2016 at the Ruukki field station to monitor the leaching of substances and GHGs from a cultivated peatland. We report results from the first two years after establishing the field. The N load in subsurface discharge waters increased upon increasing peat depth. Owing to the average and low amounts of discharge in the two years, the TN load was similar or lower than is commonly reported from mineral soils, but the proportion of NO_3^--N was lower and NH_4^+-N and Norg was higher than in mineral soils. The total P load was low, compared to thick peat and even mineral soils, because the coarse silty and clayey mineral subsoil likely effectively adsorbed P in the seepage water, the retention being more effective the thicker the mineral soil horizons are before the pore water reaches the drainage pipe. However, the proportion of dissolved PO_4-P increased upon increased peat depth. This study tentatively suggests that N and P loads transported through subsurface drainage pipes from a shallow peat field are lower than from a thick peat soil where the drainage pipes have been installed in the peat. Our results indicate that peat cover can mitigate the negative environmental impacts of AS soils by hindering the oxidation of sulfidic material, thus preventing the formation of acidity, but the required thickness of the peat cover to achieve this effect should be studied in greater detail. In cultivated peatlands, like our experimental field, the GHG emissions, and especially those of CO_2 and N_2O, are higher than in comparable mineral soils. Due to the short measurement campaign and recent establishment of the study field, the effects of peat depth or crops cannot be clearly seen from this data set. The CO_2-C emissions into the atmosphere were abundant during the monitored summer weeks, and the daily losses were equal to or higher than the amounts of TOC transported through the subsurface drainage pipes during the whole year, but N loss in the form of N_2O, at least in the summer, was small compared to N loss contained in discharge water. This study points out the diversity of cultivated peatlands and highlights the importance of their monitoring to obtain trustworthy estimates of the environmental loading in northern conditions.

CRediT authorship contribution statement

Yli-Halla: investigation, methodology, visualization, writing the original draft. **Lötjönen**: methodology, investigation, management. **Kekkonen**: investigation, management. **Virtanen**: conceptualization, visualization, writing the original draft. **Marttila**: investigation, management (soil measurements), visualization, funding acquisition. **Liimatainen**: investigation, visualization, writing the original draft (GHG), funding acquisition. **Saari**: investigation (GPR). **Mikkola**: statistical methodology and analysis. **Suomela**: conceptualization, investigation (establishment of the field). **Joki-Tokola**: conceptualization, investigation, project supervision and administration, funding acquisition. **All authors** contributed to the reviewing and editing of the manuscript.

Declaration of competing interest

The authors declare that they have no known competing financial interests or personal relationships that could have appeared to influence the work reported in this paper.

Acknowledgments

The authors thank the Council of Oulu Region for allocating funds originating from the European Regional and Development Fund (ERDF) for the design and implementation of the experimental field. The grants received in 2012–2017 were A32186, A71390 and A71403. We also thank the ERA-NET GAS program which funded the PEATWISE project in 2017–2020 (grant number 4400T-102), Kone Foundation for a financial support in 2018–2022 (grant number 201802192) and Suoviljelysyhdistys ry – Finnish Peat Cultivation Association for financial support in 2019–2021. The authors thank professor Kristiina Regina, Natural Resources Institute Luke, Finland, for organizing the GHG measurement campaign and the respective analyses.

Appendix A. Supplementary data

Supplementary data to this article can be found online at https://doi.org/10.1016/j.scitotenv.2021.150499.

References

Äijö, H., Paasonen-Kivekäs, M., Myllys, M., Nurminen, J., Turunen, M., Salo, H., Warsta, L., Koivusalo, H., Sikkilä, M., Alakukku, L., Puustinen, M., 2016. The effect of additional subsurface drainage on water discharge and nutrient load on clay soil. In: Strock, J.F. (Ed.), Proceedings of the 10th International Drainage Symposium, 7-9 Sept., 2016 Minneapolis, Minnesota. American Society of Agricultural and Biological Engineers ASABE, St Joseph, Minnesota, USA.

AnaEE, 2021. European network of platforms for analysis and experimentation on ecosystems. https://platforms.anaee.eu/research-platform-index/10052-5/.

Bärlund, I., Tattari, S., Yli-Halla, M., Åström, M., 2004. Effects of sophisticated drainage techniques on groundwater level and drainage water quality on acid sulfate soils: final report of the HAPSU project. Finn. Environ. 732, 1–68. https://helda.helsinki.fi/handle/10138/40557.

Batjes, N.H., 1996. Total carbon and nitrogen in the soils of the world. Eur. J. Soil Sci. 47, 151–163.

Berglund, Ö., Berglund, K., 2010. Distribution and cultivation intensity of agricultural peat and gyttja soils in Sweden and estimation of greenhouse gas emissions from cultivated peat soils. Geoderma 154, 173–180.

Beucher, A., Fröjdö, S., Österholm, P., Auri, J., Martinkauppi, A., Edén, P., 2015. Assessment of acid sulfate soil mapping utilizing chemical indicators in recipient waters. Bull. Geol. Soc. Finl. 87, 5–23.

Brunet, R.C., Garcia-Gil, L.J., 1996. Sulfide-induced dissimilatory nitrate reduction to ammonia in anaerobic freshwater sediments. FEMS Microbiol. Ecol. 21, 131–138.

Buschmann, C., Röder, N., Berglund, K., Berglund, O., Lærke, P.E., Maddison, M., Mander, U., Myllys, M., van den Osterburg, B., Akker, J.J.H., 2020. Perspectives on agriculturally used drained peat soils: comparison of the socioeconomic and ecological business environments of six European regions. Land Use Policy 90 13 pp.

Chen, X., Bechmann, M., 2019. Nitrogen losses from two contrasting agricultural catchments in Norway. R. Soc. Open Sci. 6 (190490). https://doi.org/10.1098/rsos.190490.

Cook, F., Dobos, S., Carlin, G., Millar, G., 2004. Oxidation rate of pyrite in acid sulfate soils: in situ measurements and modelling. Aust. J. Soil Res. 42, 499–507.

Dore, J.E., Houlihan, T., Hebel, D.V., Tien, G., Tupas, L., Karl, D.M., 1996. Freezing as a method of sample preservation for the analysis of dissolved inorganic nutrients in seawater. Mar. Chem. 53, 173–185.

Duxbury, J.M., Beverly, J.H., 1978. Nitrogen and phosphorus losses from organic soils. J. Environ. Qual. 7, 566–570.

Edén, P., Weppling, K., Jokela, S., 1999. Natural and land-use induced load of acidity, metals, humus and suspended matter in lestijoki, a river in western Finland. Boreal Environ. Res. 4, 31–43.

Eriksen, J., Askegaard, M., 2000. Sulfate leaching in an organic crop rotation on sandy soil in Denmark. Agric. Ecosyst. Environ. 78, 107–114.

Esala, M.J., 1995. Changes in the extractable ammonium-nitrogen and nitrate-nitrogen contents of soil samples during freezing and thawing. Commun. Soil Sci. Plan. 26, 61–68.

Fellman, J.B., D'Amore, D.V., Hood, E., 2008. An evaluation of freezing as a preservation technique for analyzing dissolved organic C, N and P in surface water samples. Sci. Total Environ. 392, 305–312.

Finnish Meteorological Institute, 2021. Ilmasto. https://www.ilmatieteenlaitos.fi/ilmasto.

Griffin, R.A., Jurinak, J.J., 1973. Estimation of activity coefficients from the electrical conductivity of natural aquatic systems and soil extracts. Soil Sci. 116, 26–30.

GTK, 2021. Geological Survey of Finland. Data sets and on-line services. Acid sulfate soils. https://gtkdata.gtk.fi/hasu/index.html.

Heiderscheidt, E., 2016. Evaluation and Optimisation of Chemical Treatment for Non-point Source Pollution Control Purification of Peat Extraction Runoff Water. 580. University of Oulu Graduate School; University of Oulu, Faculty of Technology Acta Univ. Oul. C.

Heikinheimo, M., Fougstedt, B., 1992. Statistic of Soil Temperature in Finland 1971–1990. 22. Finnish Meteorological Institute. Meteorol. Publ. Finland.

Heikkinen, K., Karppinen, A., Karjalainen, S.M., Postila, H., Hadzic, M., Tolkkinen, M., Marttila, H., Ihme, R., Kløve, B., 2018. Long-term purification efficiency and factors affecting performance in peatland based treatment wetlands: an analysis of 28 peat extraction sites in Finland. Ecol. Eng. 117, 153–164.

Herzog, S.D., Persson, P., Kvashnina, K., Kritzberg, E.S., 2020. Organic iron complexes enhance iron transport capacity along estuarine salinity gradients of Baltic estuaries. Biogeosciences 17, 331–344. https://doi.org/10.5194/bg-17-331-2020.

Huhta, H., Jaakkola, A., 1993. Viljelykasvin ja lannoituksen vaikutus ravinteiden huuhtoutumiseen turvemaasta Tohmajärven huuhtoutumiskentällä v. 1983-87. Maatalouden tutkimuskeskus. Tiedote 20/93.

Ingri, J., Conrad, S., Lidman, F., Nordblad, F., Engström, E., Rodushkin, I., Porcelli, D.J., 2018. Iron isotope pathways in the boreal landscape: role of the riparian zone. Geochim. Cosmochim. Acta 239, 49–60. https://doi.org/10.1016/j.gca.2018.07.030.

IPCC, 2014. In: Hiraishi, T., Krug, T., Tanabe, K., Srivastava, N., Baasansuren, J., Fukuda, M., Troxler, T.G. (Eds.), 2013 Supplement to the 2006 IPCC Guidelines for National Greenhouse Gas Inventories: Wetlands. IPCC, Switzerland.

ISO 11905-1:1997, 1997. Water Quality — Determination of Nitrogen — Part 1: Method Using Oxidative Digestion With Peroxodisulfate. International Organization for Standardization.

IUSS Working Group WRB, 2014. World Reference Base for Soil Resources 2014. World Soil Resources Reports 106. FAO, Rome.

Ivarson, K.C., 1977. Changes in decomposition rate, microbial population and carbohydrate content of an acid peat bog after liming and reclamation. Can. J. Soil Sci. 57, 129–137.

Jaakkola, A., 1984. Leaching losses of nitrogen from a clay soil under grass and cereal crops in Finland. Plant Soil 76, 59–66.

Kaila, A., 1959. Retention of phosphate by peat samples. J. Sci. Agric. Soc. Finl. 31, 215–225.

Kaiser, M., Kleber, M., Berhe, A.A., 2015. How air-drying and rewetting modify soil organic matter characteristics: an assessment to improve data interpretation and inference. Soil Biol. Biochem. 80, 324–340.

Kasimir-Klemedtsson, Å., Klemedtsson, L., Berglund, K., Martikainen, P., Silvola, J., Oenema, O., 1997. Greenhouse gas emissions from farmed organic soils: a review. Soil Use Manag. 13, 245–250.

Kekkonen, H., Ojanen, H., Haakana, M., Latukka, A., Regina, K., 2019. Mapping of cultivated organic soils for targeting greenhouse gas mitigation. Carbon Manag. 10 (2), 115–126. https://doi.org/10.1080/17583004.2018.1557990.

Kenward, M.G., Roger, J.H., 2009. An improved approximation to the precision of fixed effects from restricted maximum likelihood. Comput. Stat. Data Anal. 53, 2583–2595.

Kersalo, J., Pirinen, P., 2009. Suomen maakuntien ilmasto. Abstract: The Climate of Finnish Regions. 8. Finnish Meteorol. Inst. Rep.

Kløve, B., Sveistrup, T.E., Hauge, A., 2010. Leaching of nutrients and emission of greenhouse gases from peatland cultivation at Bodin, northern Norway. Geoderma 154, 219–232.

Lohila, A., Aurela, M., Regina, K., Laurila, T., 2003. Soil and total ecosystem respiration in agricultural fields: effect of soil and crop type. Plant Soil 251, 303–317.

Longabucco, P., Rafferty, M.R., 1989. Delivery of nonpoint-source phosphorus from cultivated mucklands to Lake Ontario. J. Environ. Qual. 18, 157–163.

Maljanen, M., Hytönen, J., Mäkiranta, P., Alm, J., Minkkinen, K., Laine, J., Martikainen, P.J., 2007. Greenhouse gas emissions from cultivated and abandoned organic croplands in Finland. Boreal Environ. Res. 12, 133–140.

Manninen, N., Soinne, H., Lemola, R., Hoikkala, L., Turtola, E., 2018. Effects of agricultural land use on dissolved organic carbon and nitrogen in surface runoff and subsurface drainage. Sci. Total Environ. 618, 1519–1528.

Mattsson, T., Kortelainen, P., Räike, A., 2005. Export of DOM from boreal catchments: impacts of land use cover and climate. Biogeochemistry 76, 373–394.

Myllys, M., Sinkkonen, M., 2004. Viljeltyjen turve- ja multamaiden pinta-ala ja alueellinen jakauma suomessa. Summary: the area and distribution of cultivated organic soils in Finland. Suo – Peat Mires 55, 53–60.

Nieminen, M., Jarva, M., 1996. Phosphorus adsorption by peat from drained mires in southern Finland. Scand. J. For. Res. 11, 321–326.

Nykänen, H., Alm, J., Lång, K., Silvola, J., Martikainen, P.J., 1995. Emissions of CH4, N2O and CO2 from a virgin fen and a fen drained for grassland in Finland. J. Biogeogr. 22, 351–357.

Nystrand, M., Auri, J., Bollström, F., Hadzic, M., Ihme, R., Österholm, P., 2019. Minimum peat thickness to prevent oxidation of underlying sulfidic mineral soil in peat extraction sites. Geophys. Res. Abstr. 21, EGU2019-8066.

Österholm, P., Åström, M., 2004. Quantification of current and future leaching of sulfur and metals from boreal acid sulfate soils, western Finland. Aust. J. Soil Res. 42, 547–551.

Purokoski, P., 1959. Rannikkoseudun rikkipitoisista maista. Referat: Über die schwefelhaltigen Böden an der Küste Finlands. 74. Agrogeological Publ, Helsinki, Finland.

Regina, K., Syväsalo, E., Hannukkala, A., Esala, M., 2004. Fluxes of N2O from farmed peat soils in Finland. Eur. J. Soil Sci. 55, 591–599.

Regina, K., Pihlatie, M., Esala, E., Alakukku, L., 2007. Methane fluxes on boreal arable soils. Agric. Ecosyst. Environ. 119, 346–352.

Regina, K., Heikkinen, J., Maljanen, M., 2019. Greenhouse gas fluxes in agricultural soils in Finland. In: Shurpali, N., Agarwal, A.K., Srivastava, V.K. (Eds.), Greenhouse Gas Emissions: Challenges, Technologies and Solutions. Book Series Energy, Environment and Sustainability. Springer, pp. 7–22.

Richards, L.A., 1954. Diagnosis and improvement of saline alkali soils. Agriculture Handbook. 60. US Department of Agriculture, Washington DC.

Ronkanen, A.-K., Marttila, H., Celebi, A., Kløve, B., 2016. The role of aluminium and iron in phosphorus removal by treatment. Ecol. Eng. 86, 190–201.

Saarela, I., 2008. Estimating bioavailable reserves and potential leaching of soil P by simple chemical tests. NJF Seminar Phosphorus Management in Nordic-Baltic Agriculture – Reconciling Productivity and Environmental Protection. NJF Reports. 4, 4 , pp. 166–170. https://orgprints.org/15044/1/njffosfor.pdf.

Sandmeier, K.J., 2016. ReflexW (Computer Software). Sandmeier Software . https://www.sandmeier-geo.de/.

Scharlemann, J.P.W., Tanner, E.V.J., Hiederer, R., Kapos, V., 2014. Global soil carbon: understanding and managing the largest terrestrial carbon pool. Carbon Manag. 5, 81–91.

SFS 3005: 1981, 1981. Veden alkaliteetin ja asiditeetin määritys. Potentiometrinen titraus. (Determination of the Alkalinity and Acidity of Water. Potentiometric Titration). Finnish Standards Association.

SFS 3021:1979, 1979. Veden pH-arvon määritys. (Determination of the pH of Water). Finnish Standards Association.

SFS-EN 1484: 1997, 1997. Water Analysis. Guidelines for the Determination of Total Organic Carbon (TOC) and Dissolved Organic Carbon (DOC). Finnish Standards Association.

SFS-EN 27888:en, 1994. Water Quality. Determination of Electrical Conductivity (ISO 7888:1985). Finnish Standards Association.

SFS-EN ISO 11732:en, 2005. Water Quality. Determination of Ammonium Nitrogen. Method by Flow Analysis (CFA and FIA) and Spectrometric Detection (ISO 11732: 2005). Finnish Standards Association.

SFS-EN ISO 11885:2009, 2009. Water Quality. Determination of Selected Elements by Inductively Coupled Plasma Optical Emission Spectrometry (ICP-OES) (ISO 11885: 2007).

SFS-EN ISO 13395:en, 1997. Water Quality. Determination of Nitrite Nitrogen and Nitrate Nitrogen and the Sum of Both by Flow Analysis (CFA and FIA) and Spectrometric Detection (ISO 13395:1996). Finnish Standards Association.

SFS-EN ISO 15681-1:2005, 2005. Water Quality. Determination of Orthophosphate and Total Phosphorus Contents by Flow Analysis (FIA and CFA). Part 1: Method by Flow Injection Analysis (FIA) (ISO 15681-1:2003).

Šimek, M., Virtanen, S., Krištůfek, V., Simojoki, A., Yli-Halla, M., 2011. Evidence of rich microbial communities in subsoil of boreal acid sulfate soil conducive to greenhouse gas emissions. Agric. Ecosyst. Environ. 140, 113–122.

Sippola, J., 1974. Mineral composition and its relation to texture and to some chemical properties in Finnish subsoils. Ann. Agric. Fenn. 13, 169–234.

Soil Survey Staff, 2014. Keys to Soil Taxonomy. 12th ed. USDA-Natural Resources Conservation Service, Washington, DC.

Soini, S., Virri, K., 1968. Soil map of Oulu-Liminka. Ann. Agric. Fenn. 7 (Suppl. 2).

Soveri, J., Varjo, M., 1977. Roudan muodostumisesta ja esiintymisestä Suomessa vuosina 1955-1975. English summary: On the formation and occurrence of frost in Finland 1955-1975. Publ. Water Environ. Res. Inst. 20.

Syväsalo, E., Regina, K., Turtola, E., Lemola, R., Esala, M., 2006. Fluxes of nitrous oxide and methane, and nitrogen leaching from organically and conventionally cultivated sandy soil in western Finland. Agric. Ecosyst. Environ. 113, 342–348.

Tattari, S., Koskiaho, J., Kosunen, M., Lepistö, A., Linjama, J., Puustinen, M., 2017. Nutrient loads from agricultural and forested areas in Finland from 1981 up to 2010 - can the efficiency of undertaken water protection measures seen? Environ. Monit. Assess. 189 (95). https://doi.org/10.1007/s10661-017-5791-z.

Tikkanen, M., Oksanen, J., 2002. Late weichselian and holocene shore displacement history of the Baltic Sea in Finland. Fennia 180, 9–20.

Tubiello, F.N., Biancalani, R., Salvatore, M., Rossi, S., Conchedda, G., 2016. A worldwide assessment of greenhouse gas emissions from drained organic soils. Sustainability - Basel 371 (8). https://doi.org/10.3390/su8040371 13 pp.

Turtola, E., Jaakkola, A., 1986. Viljelykasvin, lannoituksen ja sadetuksen vaikutus kaliumin, kalsiumin, magnesiumin, natriumin, sulfaattirikin sekä kloridin huuhtoutumiseen savimaasta. Maatalouden tutkimuskeskus. Tiedote 17/1986.

Turtola, E., Paajanen, A., 1995. Influence of improved subsurface drainage on phosphorus losses and nitrogen leaching from a heavy clay soil. Agric. Water Manag. 28, 295–310.

Urvas, L., 1976. Soil map of Ruukki-Lumijoki. Ann. Agric. Fenn. 15 (Suppl. 1).

Vuorinen, J., Mäkitie, O., 1955. The Method of Soil Testing in Use in Finland. 63. Agrogeological Publ, Helsinki, Finland, pp. 1–14.

Yli-Halla, M., Puustinen, M., Koskiaho, J., 1999. Area of cultivated acid sulfate soils in Finland. Soil Use Manag. 15, 62–67.

Yli-Halla, M., Virtanen, S., Mäkelä, M., Simojoki, A., Hirvi, M., Innanen, S., Mäkelä, J., Sullivan, L., 2017. Abundant stocks and mobilization of elements in boreal acid sulfate soils. Geoderma 308, 333–340.

Yli-Halla, M., Virtanen, S., Regina, K., Österholm, P., Ehnvall, B., Uusi-Kämppä, J., 2020. Nitrogen stocks and flows in an acid sulfate soil. Environ. Monit. Assess. 192 (751).